Aspects of Particle Physics and Cosmology from String/M Theory

Pongkitivanichkul, Chakrit

Awarding institution:
King's College London

King's College London

Doctoral Thesis

Aspects of Particle Physics and Cosmology from String/M theory

Author:

Chakrit Pongkitivanichkul

Supervisor:

Prof. Bobby Samir Acharya

A thesis summitted in fulfilment of the requirements
for the degree of Doctor of Philosophy
in the
Theoretical Particle Physics and Cosmology Group
Department of Physics

August 14, 2016

Contents

Acknowledgements

I would like to express my deepest gratitude to my supervisor Professor Bobby Acharya for guiding me to a wide range of research opportunities and collaborations. Without his continually support and encouragement, this thesis would not have been possible. I would like to also thank to all my colleagues: Professor Stephen King, Kazuki Sakurai, Miguel Crispim Romao, and especially Krzystof Bozek for their helpful discussion and collaborations. Also, I would like to thank to all graduate/postdocs friends at King's College London for invaluable assistance and support. I would never forget all beautiful moments with my friends at King's. I am very grateful to Professor Veronica Sanz and Professor Alexander Belyaev for their time and effort on providing constructive feedback of the thesis. Finally, and most importantly, I would like to thank my family for their persistent support and unconditional love throughout my life.

Abstract

This thesis is focused on various aspects of particle physics and cosmology from String/M theory. Assuming our universe is a solution of string/M theory, physics below the unification scale is an effective 4D supergravity theory with an abundance of moduli and axions. The phenomenology of moduli and axions in an early universe is studied. We particularly study dark radiation constraints on a generic Axiverse scenario and provide various solutions to it. The simplest solution requires the lightest modulus decays only into its own axion superpartner and this severely constrains the moduli Kahler potential and mass matrix. We also study a model building aspect of string/M theory. It has been shown that a discrete symmetry on a manifold with G_2 holonomy combined with symmetry breaking Wilson lines provide a solution to the doublet-triplet splitting problem. We extend the idea to a new class of model based on M theory compactified on a G_2 manifold which leads to a novel solution where the colour triplets are decoupled. The models also involves an extra vector-like standard model multiplet to restore gauge unification. We will also discuss the phenomenology of the new light states and the induced R-parity violation. We will also study the prospects of searches from a future generation of colliders. We focus in particular on the search at a 100 TeV collider via the WZ channel. The motivation from string/M theory models leads to the assumption that Higgsinos form the lightest supersymmetric particle. We design simple signal regions for the trilepton channel and find that neutralinos-charginos could be discovered(excluded) up to 1.1 (1.8) TeV.

Chapter 1

Introduction

Quantum Field Theory (QFT) is a mathematical framework which describes the quantum behaviour of the physical system consistently with special relativity. Depending on the symmetry properties, interactions, and particle content, QFT can be used to describe a wide range of physical systems such as elementary particles and condensed matter. One particular example is the standard model of particle physics (SM) which is a QFT in 4 dimensions with $SU(3) \times SU(2) \times U(1)$ gauge symmetry. The standard model is the most successful particle physics model ever known. Its predictions confront many experimental observations at the precision of one part in a billion in some cases.

Albeit successful, there are many reasons to expect physics beyond the Standard Model (BSM) [1–11]. Experimentally, the most notorious one is the existence of dark matter and dark energy. Although there is strongly convincing yet indirect evidence for the dark sector, there is no possible candidate in the SM. Moreover, the SM offers no mechanism and ingredient for generating the neutrino masses which have been confirmed from neutrino oscillation experiments. From theoretical side, the hierarchy problem is also a strong motivation to call for BSM physics

stabilising the SM Higgs mass against quadratic divergences. Also, the SM allows non-vanishing terms that break CP symmetry of the strong interaction sector. However, strong CP violation is severely constrained experimentally by the limit from neutron electric dipole moment experiments.

One of the most well-motivated BSM theory is low energy supersymmetry (SUSY). Not only does SUSY provide an explanation to most of the puzzles we listed above, it also contains attractive features such as radiative electroweak symmetry breaking (REWSB) and gauge unification. If nature really is supersymmetric, a supersymmetric standard model with soft supersymmetry breaking could contain at least a hundred parameters waiting to be determined by future experiments. To address such questions and many more to come systematically, we need a complete theory whose low energy limit is described by supersymmetry. Such a complete theory must also be capable of providing a consistent description ranging from the cosmological scale down to the particle physics scale. So far, string/M theory is one of the leading candidates offering a solution to the consistency of quantum gravity. Similarly to QFT, string/M theory is a very broad framework. Due to recent developments in string compactification, it is possible to formulate a model with features needed to connect to low energy physics such as massive moduli fields and supersymmetry breaking with a small positive cosmological constant.

Although there might be a lot to understand from a formal perspective of string/M theory, one can still draw generic low energy predictions from the string/M framework that become interesting phenomenologically. *The goal of this thesis work is to study phenomenological consequences from a string/M theory framework and constrain them from experiments.* We will from now on assume that our universe is indeed described by a solution of string/M theory with low energy

supersymmetry and grand unification. Given this basic assumption, the physics below the grand unification scale can be described by a 4-dimensional supergravity theory. One particular distinctive feature from other supersymmetric BSM models is that particle content of the theory is not only that of the minimal supersymmetric standard model but also moduli and axions which are low energy remnants of the string compactification. The existence of these additional scalar fields is perhaps the most generic prediction from string theory framework applying to our assumption.

The moduli fields are essentially higher dimensional gravitons, i.e., massless scalar fields with Planck suppressed interactions. They arise naturally from the geometry of the extra dimensions. For example, the most common types are volume moduli and complex structure moduli which control the shape and the size of the extra dimensions. Not only do they play a role in extra dimensional space, they also connect with low energy physics directly. The crucial property of the moduli fields is that their vacuum expectation values set the low energy physical parameters such as gauge couplings and yukawa couplings. However, if the moduli fields are massless, their vacuum expectation values would not be fixed. In addition, the presence of massless scalar fields would lead to new long range forces which have not been observed in nature. This means that all moduli must be stabilised by their potential with significant masses in order to connect with real world physics. The substantial progress has been made on moduli stabilisation in various corners of string theory [12–17].

In the supergravity theory, the gravitino mass $m_{3/2}$ sets the typical scale of all scalar field masses including moduli. With this implication, the moduli play a very important role in an early universe via vacuum misalignment mechanism [18–20]. At early times, when the Hubble scale H is higher than the moduli mass, the field

is frozen due to the friction term in the equation of motion. When the universe expands and H decreases to become the order of the moduli mass, the coherent oscillation of moduli fields starts, leading to the matter-dominated universe. Since the moduli have Planck suppressed couplings, the lifetime can be approximated as $\tau = M_{pl}^2/m_{3/2}^3$. Their lifetime must be less than $\sim 10^{-1}$ second, otherwise their decay products will destroy the successful predictions of Big Bang nucleosynthesis (BBN). This is known as the cosmological moduli problem [21, 22]. This requires the limit of gravitino mass to be $m_{3/2} \gtrsim 10$ TeV. This leads to another generic prediction from string theory that the universe is matter-dominated before BBN era [23].

Although moduli can be stabilised and get heavy masses, their axionic partners which arise from Kaluza Klein (KK) zero modes of antisymmetric tensor fields in higher dimensions, are protected by shift symmetries. Similar to the QCD axion, their masses are generated from instanton effects. Since the axionic potential is generically suppressed by instanton actions, axions arising from string compactification are expected to be very light. The number of axions depends on the topological property of the compactified manifold and associated with the corresponding Betti number of the manifold [24, 25]. Many examples of compactified manifolds have been studied and the Betti number ranges from 1 to 1000 [26–28]. This leads to the notion of *the string Axiverse*, i.e., the universe filled with many ultra light axions [29].

Axions also play very significant roles in the dark sector of the universe. Similar to moduli fields, when $H \sim m_a$ axions also behave like matter. However, there is one important difference from moduli: axions have an extremely long lifetime due to their very small masses. Therefore if axions are produced non-thermally, they can be a perfect candidate for dark matter. Axions can also be an additional

component of the radiation energy density of the universe also known as dark radiation. Since moduli with mass $\sim$ TeV can decay into SM particles as well as their axion partners, axions produced from moduli decay will be relativistic. This leads to an extra component of radiation from axions whose extremely weak couplings separate them from the SM thermal bath. The dark radiation from axion is one of the generic predictions which is often constrained severely from precision cosmological observables. I will focus on the dark radiation constraints in the Axiverse scenario in this thesis.

Recently, significant progress has been made in the context of M theory compactification on a manifold with G_2 holonomy. The moduli stabilisation in this framework has been investigated in [30]. It was shown in [31, 32] that under reasonable assumptions, a G_2 compactification gives rise to the resulting $N = 1$ supergravity theory with low scale supersymmery breaking. Assuming that particle content of the visible sector to be at least that of MSSM, it provides the basis for studying phenomenological consequences in M theory framework. A study of a new class of models from M theory framework in which I made substantial contributions will form another section of the thesis.

In the rest of this chapter we will review various topics that can be useful in this thesis. We will review the origin of scalar fields from string theory. We will also review supersymmetric phenomenological models where the μ problem and R-parity violation are the main focus. Finally we will provide an outline for the thesis.

1.1 Scalar fields from string theory

We review scalar fields resulting from string compactification in this section. To give an idea, it is rather insightful to review the Kaluza Klein compactification of the original fifth dimension model as the simplest example before moving on to the string/M theory compactification on Calabi-Yau/G_2 manifold. The idea of the fifth dimension was proposed [33] in an attempt to unify electromagnetism with gravity. The 5D gravity is reduced to 4D gravity plus an abelian gauge theory if the fifth dimension is compactified on a circle which is assumed to be too small to be observed from current experiments.

1.1.1 Introduction to Compactification

The simplest example of the scalar fields from compactification is the Kaluza Klein states. Let's consider an action of a real massless scalar field in a Minkowski space with $D = 5$

$$S = \int d^5x \partial_M \phi \partial^M \phi \tag{1.1}$$

where $M = 0, \ldots, 4$ with $\eta_{MN} = diag(-, +, +, +, +)$. Assume that the fifth direction gets compactified in a circle of radius R, i.e, the 5D space is a product of $\mathcal{M}_5 = \mathcal{M}_4 \times S^1$. We write the coordinate as $x_M = (x_\mu, y)$, where $\mu = 0, 1, 2, 3$ and $y \in [0, 2\pi R]$. The equation of motion in 5D reads

$$\partial_M \partial^M \phi = \partial_\mu \partial^\mu \phi + \partial_y^2 \phi = 0 \tag{1.2}$$

Due to the periodicity of the field $\phi(x_\mu, y) = \phi(x_\mu, y + 2\pi R)$, we can expand the field in a Fourier series

$$\phi(x, y) = \frac{1}{\sqrt{2\pi R}} \sum_{n=-\infty}^{\infty} \phi_n(x) e^{iny/R}. \tag{1.3}$$

Substitute back to the equation of motion we get

$$\partial_\mu \partial^\mu \phi_n + \frac{n^2}{R^2} \phi_n = 0 \tag{1.4}$$

which means that $\phi_n(x)$ is a scalar field in 4D with mass $\frac{n}{R}$. The analysis shows that a single scalar field in higher dimension under a compactification process gives rise to an infinite tower of particles with masses $\frac{n}{R}$ where $n \in \mathbf{Z}$.

Now let's consider the gravity part of the KK compactification. The 5D Einstein Hilbert action is written as

$$S = M_5^3 \int d^5x \sqrt{-G} R_{5d} \tag{1.5}$$

where $G = det(G_{MN})$ and R_{5d} is the 5D Ricci scalar. Again we perform Fourier expansion on the metric field

$$G_{MN} = \frac{1}{\sqrt{2\pi R}} \sum_{n=-\infty}^{\infty} G_{MN}^n(x) e^{iny/R}. \tag{1.6}$$

As we see in the analysis on a scalar field, 4D theory will contain massless fields and a tower of massive states. The massless sector turns out to be the usual graviton $g_{\mu\nu}$, a vector field A_μ and a scalar field S living in the zero mode of the

5D metric as [33–35]

$$G^0_{MN} = e^{S/3} \begin{pmatrix} g_{\mu\nu} + e^{-S} A_\mu A_\nu & e^{-S} A_\mu \\ e^{-S} A_\nu & e^{-S} \end{pmatrix}. \tag{1.7}$$

S is the simplest example of the moduli field which has a vanishing potential and its vev parametrises a microscopic property which is identified as the inverse of the radius in this case.

The presence of moduli fields arising from the higher dimensional metric is generic to any compactified manifolds. This gives rise to many interesting physical consequences as we will review later on. Another instructive example is the torus $T^2 = S^1 \times S^1$ which we can identify moduli fields associated with its area and its shape as

$$S = R_1 R_2, \; U = R_2/R_1 \tag{1.8}$$

where R_1 and R_2 are inner radius and outer radius respectively.

1.1.2 Moduli and Axions from String Compactification

Although our examples so far have been illustrative, in a compactification leading to more realistic physics, a compactified manifold is typically non-trivial. In string/M theory we certainly start from a 10D or 11D maximally supersymmetric theory. Therefore the compactified manifold must break some portion of supersymmetry resulting in a preferable phenomenology. This is the main criterior for string compactifications. For example, it was found that the superstring compactification on a Calabi-Yau manifold leads to $N = 1$ supersymmetry in 4D [36]. Similar results can also be found in M-theory compactification on a manifold with G_2 holonomy [37, 38].

To analyse the more general case, the higher dimensional metric can be decomposed into $g_{MN} \to g_{\mu\nu} \oplus g_{\mu n} \oplus g_{mn}$. The zero modes from $g_{\mu\nu}$ are the lower dimensional graviton, whereas massless modes corresponding to gauge bosons come from $g_{\mu n}$. To find the moduli fields which correspond to the extra dimensional metric g_{mn}, we begin by writing a metric perturbation $g_{mn} = \widetilde{g}_{mn} + h_{mn}$. Then the moduli fields h_{mn}, which parametrises the degeneracy of the vacuum, can be found by the condition $R_{MN}(g_{mn}) = 0$. The vanishing Ricci curvature is a necessary condition for a manifold with the holonomy groups preserving supersymmetry [24, 25, 39].

For example, in G_2 manifold compactification [38], the vanishing Ricci curvature gives rise to the Lichnerowicz equation

$$\Delta_L h_{mn} \equiv -\nabla_M^2 h_{mn} - 2R_{mpnq}h^{pq} + 2R^p_{(m}h_{p)n} = 0. \tag{1.9}$$

In order to perform Kaluza Klein analysis, we write the perturbation as

$$h_{MN} = \overline{h}_{MN}(x)\rho(y) \tag{1.10}$$

where x is the 4 dimensional coordinate and y denotes coordinates in higher dimensions. If we write the covariant derivative as

$$\nabla_M^2 = \nabla_\mu^2 + \nabla_m^2, \tag{1.11}$$

we can see that the fluctuations leads to a tower of scalar fields in 4 dimensions with masses given by the eigenvectors of the Lichnerowicz operator

$$\overline{h}_{MN}\nabla_\mu^2\rho(y) = -(\Delta_L\overline{h}_{MN})\rho(y) = -\lambda\overline{h}_{MN}\rho(y) \tag{1.12}$$

Therefore, the zero modes of the Lichnerowicz operator can be identified as massless moduli fields in 4 dimensions.

From the 11D supergravity theory, there is also a 3-form field C with field strength $G = dC$. Under Kaluza Klein compactification, the 3-form field leads to a pseudoscalar field in 4D. The equation of motion is $d * G = \frac{1}{2} G \wedge G$. The pseudoscalars also known as axions can be obtained from the KK ansatz

$$C = \sum_{I=1}^{b_3(X)} \omega^I(x) t_I(y) \tag{1.13}$$

where ω^I form a basis for the harmonic 3-forms on G_2 manifold. The number of scalar fields is determined from the third betti number $b_3(X)$ which is the number of linearly independent harmonic 3-forms. It was shown that axions and moduli pair up giving $b_3(X)$ massless complex scalars fields which are the components of massless chiral superfields in 4D $N = 1$ supergravity.

1.2 Supersymmetry

Supersymmetry is a symmetry which relates fermions to bosons. From the top-down point of view, supersymmetry guarantees the absence of quadratic divergences and provides consistency in string theory. Supersymmetry also stabilises the mass of scalar fields such as Higgs boson and therefore becomes a solution to the electroweak hierarchy problem. These reasons have led to the extensive studies in the past decades on a compactification which gives supersymmetric theories at low energies.

A supersymmetry transformation turns a fermionic state into a bosonic state

and vice versa:

$$Q|\text{fermion}\rangle = |\text{boson}\rangle, \;\; Q|\text{boson}\rangle = |\text{fermion}\rangle. \tag{1.14}$$

The supersymmetry is also a spacetime symmetry. In fact supersymmetry generators, Q_α and $\overline{Q}_{\dot{\alpha}}$, which are also fermionic operators form the supersymmetry algebra

$$\{Q_\alpha, \overline{Q}_{\dot{\beta}}\} = 2\sigma^\mu_{\alpha\dot{\beta}} P_\mu, \; [M^{\mu\nu}, Q_\alpha] = i(\sigma_{\mu\nu})^\beta_\alpha Q_\beta \tag{1.15}$$

$$\{Q_\alpha, Q_\beta\} = \{\overline{Q}_{\dot{\alpha}}, \overline{Q}_{\dot{\beta}}\} = [P^\mu, Q_\alpha] = [P^\mu, \overline{Q}_{\dot{\alpha}}] = 0 \tag{1.16}$$

where P_μ and $M_{\mu\nu}$ are Poincare operators. The irreducible representations of the supersymmetry algebra are called supermultiplets. In the superfield formalism, different field components are unified into a single superfield using the notion of superspace where the Minkowski coordinates is combined with the anticommuting spinorial coordinates $\theta^\alpha, \overline{\theta}_{\dot{\alpha}}$. There are 2 types of supermultiplets required to construct the supersymmetry Lagrangian:

- The chiral superfield Φ, containing a complex scalar ϕ, a Weyl fermion ψ and an auxiliary field F. The expansion in superfield coordinates is written as

  $$\Phi(x, \theta, \overline{\theta}) = \phi(y) + \sqrt{2}\theta^\alpha \psi_\alpha(y) + \theta^\alpha \theta_\alpha F(y). \tag{1.17}$$

  where $y^\mu = x^\mu + i\theta^\alpha \sigma^\mu_{\alpha\dot{\beta}} \overline{\theta}^{\dot{\beta}}$. Notice that due to the fact that scalar fields and fermionic fields have mass dimension 1 and $\frac{3}{2}$ respectively, the spinorial coordinates have mass dimension $-\frac{1}{2}$ whereas the auxiliary field F has mass dimension 2.

- The vector superfield under the Wess-Zumino gauge consists of gauge bosons

A_μ, Weyl spinors called gauginos λ and an auxiliary field D. The expansion in superspace is

$$V(x,\theta,\overline{\theta}) = -\theta^\alpha \sigma^\mu_{\alpha\dot{\beta}} \overline{\theta}^{\dot{\beta}} A_\mu(x) + i\theta^\alpha \theta_\alpha \overline{\theta}_{\dot{\beta}} \overline{\lambda}^{\dot{\beta}}(x) - i\overline{\theta}_{\dot{\alpha}} \overline{\theta}^{\dot{\alpha}} \theta^\beta \lambda_\beta(x) + \frac{1}{2}\theta^\alpha \theta_\alpha \overline{\theta}_{\dot{\beta}} \overline{\theta}^{\dot{\beta}} D(x) \tag{1.18}$$

Notice that botht the vector superfield and the auxiliary field D have no mass dimension in total. The field strength lives in a chiral superfield defined from a vector superfield:

$$W_\alpha = \frac{1}{4} \overline{D}_{\dot{\beta}} \overline{D}^{\dot{\beta}} e^{-V} D_\alpha e^V \tag{1.19}$$

where D's denote the supersymmetric covariant derivatives.

1.2.1 The Supergravity Action

For the $N = 1$ supergravity, the supersymmetry transformation which is promoted to be spacetime dependent, is proved to be invariant by introducting a gravity supermultiplet containing a spin-2 graviton and a spin-3/2 gravitino. The supergravity action is non-renormalisable and hence considered to be an effective theory with a cut off below Planck scale. A supergravity action is characterised by 3 functions:

- *The gauge kinetic function* $f(\Phi_i)$ introduces a field dependence on gauge kinetic terms. It is a holomorphic function of chiral fields. The gauge kinetic Lagrangian is given by

$$\frac{1}{4} f(\Phi_i) \mathrm{Tr} \int d^2\theta W^\alpha W_\alpha + h.c. \tag{1.20}$$

The expansions and the integration in superspaces gives a gauge kinetic term, and an axion θ term given by

$$-\frac{1}{4}\mathrm{Re}(f)F_{\mu\nu}F^{\mu\nu}-\frac{1}{4}\mathrm{Im}(f)F_{\mu\nu}\widetilde{F}^{\mu\nu} \tag{1.21}$$

The later term is central to the strong CP problem which we will explain in later chapters.

- *The Kahler potential* $K(\Phi_i,\overline{\Phi}_{\bar{i}})$ is a real function of the chiral multiplets. It has mass dimension 2 where the Lagrangian can be obtain by integrating the full superspace:

$$\int d^2\theta d^2\overline{\theta}K. \tag{1.22}$$

The role of the Kahler potential is to provide kinetic terms for both scalar and fermionic components of the chiral multiplets. It is useful to emphasise that the complex scalar of Φ recieves a non-canonical kinetic term as

$$K_{i\bar{j}}\partial_\mu\phi^i\partial^\mu\overline{\phi}^{\bar{j}},\ \text{ where } K_{i\bar{j}}\equiv\frac{\partial^2 K}{\partial\Phi^i\partial\overline{\Phi}^{\bar{j}}} \tag{1.23}$$

where $K_{i\bar{j}}$ is called the Kahler metric. We will later explore this aspect extensively in chapter 2 where the chiral superfields contains moduli/axions. The complete supergravity action is invariant under Kahler transformation

$$K(\Phi_i,\overline{\Phi}_{\bar{i}})\to K(\Phi_i,\overline{\Phi}_{\bar{i}})+F(\Phi_i)+\overline{F}(\overline{\Phi}_{\bar{i}}) \tag{1.24}$$

where $F(\Phi_i)$ is any holomorphic function of the chiral field. In the case of canonical kinetic terms, the chiral field Φ gauged under a gauge group with

the vector superfield V receives the kinetic term from

$$K = \Phi^\dagger e^V \Phi \tag{1.25}$$

- *The superpotential* $W(\Phi_i)$ is a holomorphic function with mass dimension 3. It captures interactions between chiral superfields in the model such as Yukawa couplings and fermion mass terms. The Lagrangian can be calculated from

$$\int d^2\theta W(\Phi_i) + h.c. \tag{1.26}$$

1.2.2 Renormalisable Action

To illustrate supersymmetric actions, we will consider the simplest case where the action is renormalisable. This will be useful in the case of the minimal setup in the next subsection. The renormalisable version of 3 functions is drastically simplified. The gauge kinetic function is taken to be a constant and normalised to 1. The Kahler potential will be given in the canonical form where the superpotential contains at most a cubic power in chiral fields. For a chiral field Φ gauge under a gauge group with a vector field V the most general Lagrangian is given by

$$\begin{aligned} \mathcal{L} &= \frac{1}{4}\mathrm{Tr}\int d^2\theta W^\alpha W_\alpha + h.c. \\ &\quad + \int d^2\theta d^2\overline{\theta}\Phi^\dagger e^V \Phi + \int d^2\theta W(\Phi_i) + h.c. \end{aligned} \tag{1.27}$$

After the superspace integration and integrating out auxiliary fields, the Lagrangian is written as

$$\begin{aligned}\mathcal{L} &= \mathrm{Tr}\left[-\frac{1}{4}F_{\mu\nu}F^{\mu\nu} - i\lambda\sigma^{\mu}D_{\mu}\overline{\lambda}\right] + \frac{\theta g^2}{32\pi^2}\mathrm{Tr}\left[F_{\mu\nu}\widetilde{F}^{\mu\nu}\right] \\ &+ D_{\mu}\phi D^{\mu}\phi - i\psi\sigma^{\mu}D_{\mu}\overline{\psi} + i\sqrt{2}g\overline{\phi}\lambda\psi - i\sqrt{2}g\overline{\psi\lambda}\phi \\ &- \frac{1}{2}\frac{\partial^2 W}{\partial\phi^i\partial\phi^j}\psi^i\psi^j - \frac{1}{2}\frac{\partial^2\overline{W}}{\partial\overline{\phi}^i\partial\overline{\phi}^j}\overline{\psi}^i\overline{\psi}^j \\ &- \frac{\partial W}{\partial\phi^i}\frac{\partial\overline{W}}{\partial\overline{\phi}^i} + \frac{g^2}{2}\sum_a \left|\overline{\phi}_i(T^a)^i_j\phi^j\right|^2 \end{aligned} \tag{1.28}$$

Notice that the action is completely controled by the superpotential in the case of the renormalisable action.

1.2.3 The Minimal Supersymmetric Standard Model

In order to solve the electroweak hierarchy problem, the superpartners of all the standard model particles must also be included. For all quarks and leptons who live in the chiral multiplet, there are scalar partners (squarks and sleptons) for each of them. Gauginos which are fermionic partners of SM gauge bosons is included to complete the vector multiplets. In the Higgs sector, a single doublet is not enough to construct down-type yukawa couplings due to the holomorphicity of the superpotential. This leads to 2 Higgs doublets model in the supersymmetric version of SM which also contain Higgs partners called Higgsinos. The full spectrum of particle is shown in table 1.1 and 1.2. If the theory contains only renormalisable operators, this model is called the minimal supersymmetric standard model (MSSM). The MSSM superpotential is given by

$$W_{\mathrm{MSSM}} = y_u H_u Q\overline{u} - y_d H_d Q\overline{d} - y_e H_d L\overline{e} + \mu H_u H_d \tag{1.29}$$

Field	spin 0	spin 1/2	$SU(3)_c \times SU(2)_L \times U(1)_Y$
Q	$(\widetilde{u}_L\ \widetilde{d}_L)$	$(u_L\ d_L)$	$(\mathbf{3},\mathbf{2},\frac{1}{6})$
$\overline{u}$	$\widetilde{u}_R$	u_R	$(\overline{\mathbf{3}},\mathbf{1},-\frac{2}{3})$
$\overline{d}$	$\widetilde{d}_R$	d_R	$(\overline{\mathbf{3}},\mathbf{1},\frac{1}{3})$
L	$(\widetilde{\nu}\ \widetilde{e}_L)$	$(\nu\ e_L)$	$(\mathbf{1},\mathbf{2},-\frac{1}{2})$
$\overline{e}$	$\widetilde{e}_R$	e_R	$(\overline{\mathbf{1}},\mathbf{1},1)$
H_u	$(H_u^+\ H_u^0)$	$(\widetilde{H}_u^+\ \widetilde{H}_u^0)$	$(\mathbf{1},\mathbf{2},\frac{1}{2})$
H_d	$(H_d^0\ H_d^-)$	$(\widetilde{H}_d^0\ \widetilde{H}_d^-)$	$(\mathbf{1},\mathbf{2},-\frac{1}{2})$

Table 1.1: Chiral multiplets in MSSM

Name	spin 1/2	spin 1	$SU(3)_c \times SU(2)_L \times U(1)_Y$
gluons, gluinos	$\widetilde{g}$	g	$(\mathbf{8},\mathbf{1},0)$
W bosons, winos	$\widetilde{W}^{\pm}$, $\widetilde{W}^0$	$W^{\pm}, W^0$	$(\mathbf{1},\mathbf{3},0)$
B boson, binos	$\widetilde{B}^0$	B^0	$(\mathbf{1},\mathbf{1},0)$

Table 1.2: Vector multiplets in MSSM

where family indices are suppressed.

Since supersymmetry implies that a particle has the same mass as its partner and such a partner of any standard model particle has not been observed yet, this motivates us for breaking supersymmetry. In general the effect of supersymmetry breaking can be parametrised by introducting extra terms called *soft terms*. In order to keep the hierarchy between the weak scale and the Planck scale, the soft terms are only allowed to break supersymmetry but not re-introduce the quadratic divergences to scalar masses. All possible soft terms in MSSM is given by [40–42]

$$\begin{aligned}
\mathcal{L} \;=\; & -\frac{1}{2}\left(M_3\widetilde{g}\widetilde{g} + M_2\widetilde{W}\widetilde{W} + M_1\widetilde{B}\widetilde{B} + c.c.\right) \\
& -\left(a_u\widetilde{u}\widetilde{Q}H_u - a_d\widetilde{d}\widetilde{Q}H_d - a_e\widetilde{e}\widetilde{L}H_d + c.c.\right) \\
& -m_{\widetilde{Q}}^2\widetilde{Q}^\dagger\widetilde{Q} - m_{\widetilde{L}}^2\widetilde{L}^\dagger\widetilde{L} - m_{\widetilde{u}}^2\widetilde{u}^\dagger\widetilde{u} - m_{\widetilde{d}}^2\widetilde{d}^\dagger\widetilde{d} - m_{\widetilde{e}}^2\widetilde{e}^\dagger\widetilde{e} \\
& -m_{H_u}^2H_u^*H_u - m_{H_d}^2H_d^*H_d - (B\mu H_uH_d + c.c.)
\end{aligned} \tag{1.30}$$

which consists of the gaugino masses M_1, M_2, M_3, trilinear coupling a_u, a_d, a_e and scalar masses squared m_j^2 and $B\mu$. Supersymmetry is clearly broken since the soft terms give masses to all scalar partners and gauginos of MSSM but not to SM particles.

Apart from the superpotential in 1.29, there are other operators that are allowed by gauge symmetries. However, they are not included because they lead to the violation of the baryon number and the lepton number. In general they are the following terms:

$$W_{\not L} = \lambda LLe + \lambda' LQ\overline{d} + \mu' LH_u \tag{1.31}$$

$$W_{\not B} = \lambda'' \overline{u}\overline{d}\overline{d} \tag{1.32}$$

where family indices are understood and being omitted. The result of the theory containing these operators leads to the proton decay problem. If both λ and λ' are significant, the proton decay rate would be too large and make protons unstable. Assuming squark masses are $\sim$ TeV, the rough estimation for proton decay width is

$$\Gamma_p \approx |\lambda\lambda'|^2 \frac{m_p^5}{m_{\tilde{q}}^4} \tag{1.33}$$

which typically gives lifetime of the proton to be many order of magnitude below 1 second unless λ and λ' were suppressed. This result strongly contradicts with the current experimental lower limit of 10^{33} years. To prevent such a problem in the MSSM, a new symmetry called *R-parity* is introduced. R-parity is a global symmetry Z_2 with the quantum number defined as

$$P_R = (-1)^{3(B-L)+2s} \tag{1.34}$$

where s is the spin of the particle. This symmetry clearly solves proton decay problem since it forbids $W_{\not L}$ and $W_{\not B}$ while maintaining $W_{\rm MSSM}$. The important consequence is that all standard model particles and Higgs bosons have $P_R = 1$ where all squarks, sleptons, gauginos and Higgsinos have $P_R = -1$. As a result, R-parity also leads to the stability of the lightest supersymmetric particle (LSP). If the LSP does not have an electric charge, it could be a perfect candidate for dark matter. The breaking of R-parity which induces proton decay and LSP decay is one of the main concerns for the model building aspect of particle physics. We will discuss this issue in more detail later.

Although the construction of the MSSM is aimed to solve the hierarchy problem, the MSSM still suffers from another naturalness problem. Analysing the Higgs potential and requiring an electroweak scale ~ 100 GeV leads to the constraint on 2 mass scales of MSSM parameter: μ and $m^2_{\rm soft} \sim m^2_{H_u}, m^2_{H_d}$. Namely, they must be fine-tuned to stay within an order of magnitude of the electroweak scale. Since there is no theoretical reason to expect μ which is supersymmetry preserving parameter being accidentally close to the values of supersymmetry breaking parameters, this is a fine-tuning problem also known as the μ problem. Several solutions have been proposed such as the Kim-Nilles mechanism [43] and the Giudice-Masiero mechanism [44]. While various solutions are different in detail, they all generically propose an extension of MSSM to include a new field and a discrete symmetry. The μ term is assumed to vanish at tree level due to the discrete symmetry then non-renormalisable operators regenerate back μ from the additional field that breaks the discrete symmetry. A similar idea can also be found in various corners of string compatifications [45]. This idea will be revisited again in chapter 3.

1.3 Thesis Outline

This thesis is organised as following. In chapter 2 based on the publication [46], we will describe the origin of moduli and axions from a string/M theory framework. We will motivate the Axiverse scenario and study its phenomenologies. In particular, we will focus on dark radiation which is significantly constrained by experiments. We will show the detailed analyses of dark radiation coming from the Axiverse and propose some possible solutions. It will be shown that the simplest solution requires the lightest modulus decays only into its own axion superpartner and this severely constrains the moduli Kahler potential and mass matrix.

In chapter 3 based on the publication [47], we will review the basic idea of the models based on M theory compactified on a G_2 manifold. Then we will review Witten's proposal on the discrete symmetry as a solution to the doublet-triplet splitting. The solution to μ problem in the framework will be also studied. We will present the construction of the new set of models based on GUT group $SO(10)$ which leads to a novel solution where the colour triplets are decoupled. The model also involves an extra vector-like Standard model family to restore gauge unification. We will also discuss about the phenomenology of the new light states and the induced R-parity violation.

In chapter 4 based on the publication [48], we will complement the thesis by a study from the bottom-up approach. We will present the prospects for discovering charginos and neutralinos at a future collider which has been discussed recently. We will focus in particular on the search at a 100 TeV collider with 3000 fb$^-$1 luminosity via the WZ channel. The motivation from string/M theory models leads to the assumption that Higgsinos form the lightest supersymmetric particle where Winos form the second lightest supersymmetric particle. We design simple but effective signal regions for the trilepton channel and find that neutralinos-

chargino could be discovered (excluded) up to 1.1 (1.8) TeV.

Chapter 2

Axiverse Dark Radiation

2.1 Introduction

2.1.1 Scalar fields from string theory

String/M theory is mathematically consistent in a 10-dimensional or 11-dimensional space-time. In order to obtain low-energy physics in 4-dimensional space-time, the extra dimensions must be compact and very small in size which is inaccessible by the current energy scale. Although the effective theory in 4 dimensions may differ in many ways depending on the details in which the extra dimensions is compactified, the existence of extra scalar fields, known as *modulus*, is generic. For example, the common type of moduli that appear naturally from the geometry are volume moduli and complex structure moduli. They are fields that parametrise the extra-dimension metric and complex structure of the compactified manifold: they control the size and the shape of the extra dimensions. Due to the complexity of the topology required to give a real world physics [16], we often find that string compactification typically gives rise to a large number of moduli $\sim \mathcal{O}(100)$. In the 4-dimension effective field theory limit the moduli simply become scalar

fields with gravitational-strength interactions, i.e., they are essentially gravitons from the extra dimensions.

The crucial aspect of moduli is that they make a direct contact with low energy physics. Let's consider interactions such as

$$\frac{s}{m_{pl}} F_{\mu\nu}^2, \text{ or } \frac{s}{m_{pl}} \overline{\psi} \not{\partial} \psi \tag{2.1}$$

where s is a modulus field. If the modulus is massless, these interactions lead to a long range force which has not been observed yet. Therefore, the mechanism for stabilising moduli fields, i.e., giving them a potential, is necessary. Moduli stabilisation also gives rise to low-energy physical parameters through their vacuum expectation values. For example, the above Lagrangian give rises to the Maxwell term, $L = \frac{1}{4e^2} F_{\mu\nu}^2$ where the electromagnetic coupling is completely determined by a modulus vev as $e^2 = \frac{s}{4m_{pl}}$. In fact, all physical quantities are determined by modulus vevs in a similar fashion.

Now let us consider the complex partners of the moduli fields from string theory – axions. The axions arise in string theory as Kaluza Klein (KK) zero modes of antisymmetric tensor fields. The fact that moduli and axions pair up to form a chiral supermultiplet implies that the number of axions in 4D theory has topological origin and is expected to be of an order $\mathcal{O}(100)$. Although moduli receive the mass from moduli stabilisation, axions is typically massless because of the shift symmetry which is a remnant of the higher-dimensional gauge invariance of the tensor fields. However, there are plenty of string instantons other than the QCD one that break shift symmetries and generate potential to axions. The axion

effective lagrangian can be parametrised as

$$\mathcal{L} = \frac{1}{2} f_a^2 (\partial\theta)^2 - \sum_i \Lambda_i^4 U_i(\theta) \tag{2.2}$$

where f_a is an axion decay constant which is typically of order the compactification scale, Λ is the energy scale generated from instanton effect, and $U(\theta)$ is a periodic function. If we assume supersymmetry breaking below the Planck scale, the overall energy scale is generated from the interference between instanton and supersymmetry breaking sources as $\Lambda^4 \sim M_{pl}^2 m_{\text{susy}}^2 e^{-S_{\text{inst}}}$. Then the mass of axions is determined by [49, 50]

$$m_a^2 = \frac{M_{pl}^2 m_{susy}^2}{f_a^2} e^{-S_{\text{inst}}} \tag{2.3}$$

We can see that, because of the exponential factor from instanton actions, axions are expected to be very light and distributed over many orders of magnitude.

Note that moduli can be stabilised by the same set of the superpotentials where the supersymmetry breaking terms are mainly responsible for generating potential for moduli. Another important point is that in order to stabilise axions, one requires the superpotential to contain as many independent terms as there are axions present in the theory. This requirement is easy to fulfill when the number of supersymmetric cycles in the compactification is large enough [50].

The axions from string theory can also play a significant role in solving the strong CP problem. The QCD gauge invariance allows a topological term in the Lagrangian.

$$\mathcal{L} = \frac{g_s^2}{4\pi} \frac{\theta_{QCD}}{8\pi} F_{\mu\nu} \tilde{F}^{\mu\nu} \tag{2.4}$$

Since quarks are massive so that there is no $U(1)_A$ to rotate the term away, the strong CP-violating θ_{QCD} parameter is physical. This can be observed from the

electric dipole moment of the neutron and the measurements gives the upper bound $\theta_{QCD} < 10^{-10}$. The axion provides an explanation why θ_{QCD} is so small. Similar to the Maxwell term from moduli coupling, there will be an axion-QCD instanton interaction term:

$$\frac{a}{f_a} F_{\mu\nu} \tilde{F}^{\mu\nu} \tag{2.5}$$

which promotes the θ_{QCD} parameter from QCD topological term into a dynamical field. When the axion is stabilised around its minimum $\theta_{QCD} = 0$ which is consistent with the experiment.

The decay constants are constrained from many experiments. The cooling process of stars and supernovae due to axion emission lead to an upper bound on axionic interaction and hence a lower bound $f_a > 10^9$ GeV. The upper bound comes from the over production of the axion as a dark matter which we will review in the next subsection.

2.1.2 Moduli and Axions in an early universe

Extremely weakly coupled scalar fields like moduli and axions can have a considerable impact on cosmological dynamics due to the "vacuum misalignment" mechanism [18–20]. The equation of motion for a massive scalar field ϕ in the expanding universe is given by

$$\ddot{\phi} + (3H + \Gamma_\phi)\dot{\phi} + m^2\phi^2 = 0 \tag{2.6}$$

where H is the Hubble scale, m is the mass of the scalar field and Γ_ϕ is the decay width of ϕ. At very early times when $H \gg m$, the friction term dominates and the fields are frozen at order one values (m_{pl} for the moduli and f_a for the axions). Then, as the Universe expands and H decreases, when H becomes of

order$\sim m_s$ or m_a, the field starts oscillating around the minimum with a frequency of order m_s or m_a. The equation of states also oscillates around $w = 0$ and the corresponding contribution to the energy density scales as $\rho_a \propto a^{-3}$.Since moduli behave as ordinatry matter, even if the Universe was radiation dominated prior to this point, a modulus field will quickly dominate the Universe since its energy density is comparable to radiation at the onset of the oscillations. Next, when the Hubble scale reduces to be of order the modulus decay width, $\Gamma_s \sim \frac{m_s^3}{m_{pl}^2}$, the modulus field decays. For $m_s \sim$ TeV, the decay products of the moduli will reionise the nuclei produced from Big Bang Nucleosynthesis (BBN). This is known as the cosmological moduli problem [21, 22]. The problem will be avoided if $m_s \geq 30$ TeV; one could also avoid it by assuming that the Hubble scale after inflation is always smaller than m_s or if there is a late period of inflation which dilutes the moduli fields, however, both of these options require tuning and are presumably not generic. Therefore, we conclude *that string/M theory seems to predict that the early Universe prior to nucleosynthesis is matter dominated.*

The axions also participate in the vacuum misalignment mechanism but there are important differences. The axion masses are small such that their lifetimes are, unlike the moduli, generically extremely long, with lifetimes that can easily be cosmologically relevant. Hence, there will be a contribution to the energy density in the form of axion fields today, which behaves as cold dark matter.

Notice that the decay of the moduli releases a large amount of entropy which dilutes any relics which existed prior to nucleosynthesis, e.g. ten orders of magnitude dilution is typical. This significantly weakens the upper bound on the QCD axion decay constant, compared to radiation dominated Universes, to be of order 10^{15} GeV [50–53]. This effect also significantly dilutes other relics that may have formed previously, such as domain walls, monopoles or thermal WIMPs.

Another important aspect of moduli-axion physics is the dark radiation which I will describe in detail in this chapter. The moduli as extradimensional gravitons, can decay into Standard Model particles, into supersymmetric particles as well as *axions*. Since the axions are so light and the moduli have masses in the tens of TeV regime, axions produced this way will be relativistic with energies of order several TeV. The expansion of the Universe and precision cosmological observables are sensitive to the relative abundance of relativistic particles. This can be captured by the observable called N_{eff} which is "the effective number of neutrino species" defined as

$$\rho_{rad} = \rho_{e^{\pm}} + \rho_{\gamma} + N_{eff}\rho_{\nu} \tag{2.7}$$

However, N_{eff} is actually sensitive to all forms of relativistic matter, regardless of how such matter couples to the Standard Model. In that sense, N_{eff} provides a very useful probe of additional, "hidden," radiation from the sectors beyond the Standard Model. Assuming that a heavy particle such as the moduli field decays into particles from hidden and visible sectors, the extra contribution from dark radiation to N_{eff} is usually parametrised by

$$\Delta N_{eff} = \frac{43}{7}\frac{\rho_{DR}}{\rho_{rad}}\left(\frac{g^*_{T_\nu}}{g^*_{T_r}}\right)^{1/3} \tag{2.8}$$

where $g^*_{T_\nu}$, $g^*_{T_r}$ are the effective degrees of freedom at the neutrino decoupling temperature and the reheating temperature, ρ_{DR} and ρ_{rad} are the radiation energy density of the dark sector and the visible sector at the reheating temperature. The full detail calculation can be found in Appendix A.1.

The Standard Model prediction [1] for N_{eff} at the time of recombination is 3.045, whilst measurements from CMB observations by WMAP 9-year polarisation data

[1] The number is not exactly 3 due to small corrections at the time of neutrino decoupling.

[54], South Pole Telescope [55], Atacama Cosmology Telescope [56], and Planck 2015 [57] are $N_{eff} = 3.84 \pm 0.40$ (WMAP9), $N_{eff} = 3.62 \pm 0.48$ (SPT), $N_{eff} = 2.79 \pm 0.56$ (ACT), $N_{eff} = 3.15 \pm 0.23$ (Planck2015) respectively. In a sense, this is a surprising result since one might expect N_{eff} to be much, much larger naively.

So, from the perspective of string/M theory or the idea of hidden sectors more generally, the question actually becomes: *why is N_{eff} so small?*. For instance, if, as we have already argued, there are large numbers of light axions and the moduli have significant branching ratios into them, why isn't N_{eff} of order N, the number of axions? We will investigate this question in this chapter.

There have been a number of interesting prior studies on axionic dark radiation in string theory [58–68]. These papers consider examples which have very few light axions. Instead, our interest here is to the dependence of N_{eff} on the number of light axions.

2.2 The Axiverse Induced Dark Radiation Problem

We will illustrate the problem by beginning with a simple model and gradually considering more and more general (realistic) cases as we go on.

The simplest Lagrangian involving a modulus (s), an axion (t) and a gauge field strength $F_{\mu\nu}$ is arguably of the form:

$$\frac{\mathcal{L}}{m_{pl}^2} = \frac{c}{s^2}\partial_\mu s \partial^\mu s + \frac{c}{s^2}\partial_\mu t \partial^\mu t + \tilde{c} s F_{\mu\nu}F^{\mu\nu} - \widetilde{m}^2(s - s_o)^2 \tag{2.9}$$

where c and $\tilde{c}$ are constants. s_o reflects that s will have a non-zero vacuum expectation value. In our conventions, s and t are dimensionless and m_{pl} is the

Planck mass. Note that the electric charge is identified with $\frac{1}{4e^2} = \widetilde{c}s$ which will be absorbed by the normalisation of the photon field. Therefore the photon-moduli couplings do not have any effect on the calculation of ΔN_{eff}

This form of the Lagrangian arises in supersymmetric string and M theory models e.g. the universal axio-dilaton Lagrangian or the model independent axion/modulus multiplet in heterotic string compactifications [25]. From this Lagrangian we can canonically normalise the fields after setting s to its vacuum value and compute the partial decay widths

$$\Gamma(\hat{s} \to \hat{t}\hat{t}) = \frac{1}{64\pi c}\frac{m^3}{m_{pl}^2} \tag{2.10}$$

and

$$\Gamma(\hat{s} \to \gamma\gamma) = \frac{1}{64\pi c}\frac{m^3}{m_{pl}^2} \tag{2.11}$$

where $m = \frac{\widetilde{m}\langle s\rangle}{\sqrt{2}c}$ is the physical moduli mass.

The contribution to dark radiation of axion from moduli decay can be calculated from [58–60]

$$\Delta N_{eff} = \frac{43}{7}\frac{\Gamma_{axions}}{\Gamma_{visible}}\left(\frac{g^*_{T_\nu}}{g^*_{T_r}}\right)^{1/3} \tag{2.12}$$

We can take the decay of moduli into two photons as a *model* for the decay of the moduli into Standard Model particles, so this calculation gives

$$\Delta N_{eff} \sim O(1) \tag{2.13}$$

since ΔN_{eff} is given by the ratio of the decay width of the modulus decay into axions versus Standard Model particles. This illustrates the fact that the moduli couple semi-universally to all particles (as one expects, since, after all they are extra dimensional gravitons).

In this work we are interested in the case when there are a large number, N of axion/moduli multiplets, (t_i, s_i). The previous Lagrangian can then be generalised to

$$\mathcal{L} = m_{pl}^2 \sum_i \left(\frac{a_i}{s_i^2}\partial_\mu s_i \partial^\mu s_i + \frac{a_i}{s_i^2}\partial_\mu t_i \partial^\mu t_i + \tilde{a}_i s_i F_{\mu\nu}F^{\mu\nu} - \widetilde{m}_i^2(s_i^2 - \langle s_i\rangle^2)\right) \tag{2.14}$$

where a_i's are constants. This Lagrangian arises from a supergravity theory containing N chiral superfields with scalar components $z_j = t_j + is_j$ with Kahler potential $K = -3\ln V$ where $V = \Pi_i s_i^{a_i}$. This Kahler potential is a typical term which would arise in string/M theory compactifications[2]. Let us now calculate $N_{eff} \equiv N_{SM} + \Delta N_{eff}$. To do this we need to evaluate the N^2 partial decay widths $\Gamma(\hat{s_j} \to \hat{t_i}\hat{t_i})$ which can readily be calculated to be

$$\Gamma(\hat{s_j} \to \hat{t_i}\hat{t_i}) = \frac{\delta_{ij}}{64\pi}\frac{1}{a_j}\frac{m_j^3}{m_{pl}^2} \tag{2.15}$$

where $m_j = \frac{\widetilde{m}_j\langle s\rangle}{\sqrt{2a_j}}$. On the other hand we also calculate

$$\Gamma(\hat{s_j} \to \gamma\gamma) = \frac{1}{64\pi}\frac{1}{(\sum_i \widetilde{a}_i\langle s_i\rangle)^2}\frac{\widetilde{a}_j^2\langle s_j\rangle^2}{a_j}\frac{m_j^3}{m_{pl}^2} \tag{2.16}$$

which results in

$$\Delta N_{eff} = \frac{(\sum_i \widetilde{a}_i\langle s_i\rangle)^2}{\widetilde{a}_j^2\langle s_j\rangle^2} = \frac{1}{(16\pi\alpha)^2\widetilde{a}_j^2\langle s_j\rangle^2} \tag{2.17}$$

where we used the fact that the sum which appears is related to the coupling constant of the gauge theory and have set the numerical factors in equation 2.12 to one for simplicity. Important points to note about this example are:

a) *due to the diagonal mass and kinetic terms, a given modulus field* $\hat{s}_j$ *decays*

[2]In the next section we will study more concrete string/M theory examples.

only into its axion partners;

b) the moduli with the smallest masses will decay last.

When the last (and lightest) modulus decays it substantially dilutes the energy density of particles produced from previous decays of heavier moduli. Hence, in computing ΔN_{eff} we are only interested in axions produced from the lightest moduli fields.

Now, *in this particular case* α is interpreted as the fine structure constant evaluated when the moduli decay takes place just before BBN, so $16\pi\alpha$ is an order one number, *independent of* N. On the other hand, since $\frac{1}{16\pi\alpha}$ is a sum of the N terms $\widetilde{a}_j\langle s_j\rangle$, if all N terms contribute similar amounts to the sum, we would have $N_{eff} \sim N^2$ which is our first indication of the *Axiverse induced dark radiation problem*. In this particular, very special model, observational consistency requires that the value of α arises only from the modulus s_j and hence that ΔN_{eff} is order one or smaller. Let us discuss more typical models.

In much more generality, the moduli dependent kinetic terms are not of the form $\frac{a_i}{s_i^2}$; rather they will be given by more complicated functions which are *homogeneous of degree minus two*. This is because the moduli Kahler potentials in string/M theory compactifications can be written as logarithms of homogeneous functions of fixed degrees, which implies that their second derivatives are homogeneous of said degree. Thus, one has a kinetic mixing matrix K_{ij} whose entries are homogeneous of degree minus two. Before we discuss this most general case, we consider an intermediate, but instructive case: models in which the kinetic coefficients are diagonal, but arbitrary functions of degree minus two, f_i. This sort of example occurs when the Kahler potential is dominated by a single term, but which could depend on all the moduli. In this case we have, setting $m_{pl} = 1$:

$$\mathcal{L} = f_i(\partial_\mu s_i)^2 + f_i(\partial_\mu t_i)^2 + \widetilde{a}_i s_i F_{\mu\nu}^2 + \sum_i \widetilde{m}_i^2 s_i^2 \tag{2.18}$$

Normalising the fields

$$s_i = \frac{1}{\sqrt{2\langle f_i\rangle}}\hat{s}_i, \quad t_i = \frac{1}{\sqrt{2\langle f_i\rangle}}\hat{t}_i, \quad A_\mu = \frac{1}{2\sqrt{\widetilde{a}_i\langle s_i\rangle}}\hat{A}_\mu \tag{2.19}$$

gives the Lagrangian

$$\mathcal{L} = \frac{1}{2}(\partial_\mu \hat{s}_i)^2 + \frac{1}{2}(\partial_\mu \hat{t}_i)^2 + \frac{1}{4}\hat{F}_{\mu\nu}^2 + \frac{\langle \partial_j f_i\rangle}{2\sqrt{2}\sqrt{\langle f_j\rangle}\langle f_i\rangle}\hat{s_j}(\partial_\mu \hat{t}_i)^2 + \frac{\widetilde{a}_j}{4\sqrt{2\langle f_i\rangle}\widetilde{a}_i\langle s_i\rangle}\hat{s}_j\hat{F}_{\mu\nu}^2 \tag{2.20}$$

This results in

$$\begin{aligned}
\Gamma(\hat{s}_j \to \hat{t}_i\hat{t}_i) &= \frac{1}{256\pi}\frac{1}{\langle f_j\rangle}\frac{1}{\langle f_i\rangle^2}\langle \partial_j f_i\rangle^2\frac{m_j^3}{m_{pl}^2} \\
\Gamma(\hat{s}_j \to \text{Axions}) &= \frac{1}{256\pi}\left(\sum_{i=1}^{N}\frac{1}{\langle f_j\rangle}\frac{1}{\langle f_i\rangle^2}\langle \partial_j f_i\rangle^2\right)\frac{m_j^3}{m_{pl}^2} \\
\Gamma(\hat{s}_j \to \gamma\gamma) &= \frac{1}{64\pi}\frac{1}{\langle f_j\rangle}\frac{\widetilde{a}_j^2}{\left(\sum_{i=1}^{N}\widetilde{a}_i\langle s_i\rangle\right)^2}\frac{m_j^3}{m_{pl}^2}
\end{aligned} \tag{2.21}$$

where $m_j = \frac{\widetilde{m}_j}{\sqrt{2\langle f_j\rangle}}$. The key point here is the sum over N terms in the second of the above equations. If the kinetic coefficient f_i depends on s_j then s_j will be able to decay into $t_i t_i$ and, in the general case we will have N such decays producing light axions, giving

$$\boxed{\Delta N_{eff} \propto N} \tag{2.22}$$

The fact that the decay width of the lightest moduli into axions is of order N is independent of the moduli couplings to the hidden sector since it only depends on the number of fields.

It is also instructive to illustrate the N-dependence in simple examples as these demonstrate how the Axiverse induced dark radiation problem might be solved. In the first example we take all of the kinetic coefficients equal and to be given by

$$f_i = \frac{1}{\sum_k s_k^2} = \frac{1}{s_1^2 + \ldots + s_N^2} \equiv \frac{1}{S_{rms}^2} \tag{2.23}$$

The decay width of the j-th modulus to decay into the i-th axion is then

$$\Gamma(\hat{s}_j \to \hat{t}_i \hat{t}_i) = \frac{1}{64\pi} \frac{\langle s_j \rangle^2}{\langle S_{rms}^2 \rangle} \frac{m_j^3}{m_{pl}^2} \tag{2.24}$$

which implies that the total decay width of the j-th modulus to decay into axions is a sum of N terms which adds up to

$$\Gamma(\hat{s}_j \to \text{axions}) = \frac{N}{64\pi} \frac{\langle s_j \rangle^2}{\langle S_{rms}^2 \rangle} \frac{m_j^3}{m_{pl}^2} \tag{2.25}$$

By comparison, the decay width into gauge bosons is

$$\Gamma(\hat{s}_j \to \gamma\gamma) = \frac{1}{64\pi} \frac{\widetilde{a}_j^2 \langle S_{rms}^2 \rangle}{\left(\sum_{i=1}^N \widetilde{a}_i \langle s_i \rangle \right)^2} \frac{m_j^3}{m_{pl}^2} \tag{2.26}$$

which leads to

$$\Delta N_{eff}(s_j) = N \frac{\langle s_j \rangle^2}{\langle S_{rms}^2 \rangle} \frac{\left(\sum_{i=1}^N \widetilde{a}_i \langle s_i \rangle \right)^2}{\widetilde{a}_j^2 \langle S_{rms}^2 \rangle} = N \frac{\langle s_j \rangle^2}{\langle S_{rms}^2 \rangle} \frac{1}{(16\pi\alpha)^2 \widetilde{a}_j^2 \langle S_{rms}^2 \rangle} \tag{2.27}$$

Clearly, in this example, we can see that if the vev of S_{rms} is sufficiently large in (11d units) then one can suppress the axion contribution to the dark radiation density.

Finally, let us discuss the most general case. The following Lagrangian:

$$\mathcal{L} = \sum_{i=1}^{N}\sum_{j=1}^{N} C_{ij} U_{ik} s_k \partial_\mu t_j \partial^\mu t_j \tag{2.28}$$

is the most general Lagrangian coupling moduli fields to axions with two derivatives of the axion fields. Here, C_{ij} arises from diagonalising the Kahler metric K_{ij} and U_{ij}, which we have ignored until now arises from diagonalising the moduli mass matrix. We supplement this Lagrangian with typical terms coupling the moduli to Standard Model and supersymmetric particles. The Lagrangian for moduli-gauge boson interactions is

$$\mathcal{L} = \sum_{i=1}^{N} B_i U_{ik} s_k F_{\mu\nu} F^{\mu\nu} \tag{2.29}$$

and the Lagrangian for moduli-scalar kinetic interactions is

$$\mathcal{L} = \sum_{i=1}^{N} D_i U_{ik} s_k D_\mu f D^\mu f \tag{2.30}$$

Dropping numerical factors, the decay width of s_k, into various channels is:

$$\begin{aligned}
\Gamma_{\text{axions}} &= \sum_{j=1}^{N} \Gamma(s_k \to t_j t_j) \\
&= \sum_{j=1}^{N} \left(\sum_{i=1}^{N} C_{ij} U_{ik} \right)^2 \frac{m_{s_k}^3}{M_{PL}^2} \\
\Gamma_{\text{gauge particles}} &= n_G \left(\sum_{i=1}^{N} B_i U_{ik} \right)^2 \frac{m_{s_k}^3}{M_{PL}^2} \\
\Gamma_{\text{fermions/sfermions}} &= n_f \left(\sum_{i=1}^{N} D_i U_{ik} \right)^2 \frac{m_{s_k}^3}{M_{PL}^2}
\end{aligned} \tag{2.31}$$

where n_G and n_f are the numbers of gauge bosons and fermions respectively.

Even though the most general model has so many parameters, one can see that we expect $N_{eff} \propto N$:

$$\langle \Delta N_{eff} \rangle \propto \frac{\Gamma_{axions}}{\Gamma_{visible}} \propto \frac{N\langle C \rangle^2}{n_G \langle B \rangle^2 + n_f \langle D \rangle^2} \propto N \tag{2.32}$$

This arises because we expect the mean values C, B and D to be comparable and that $(\sum_{i=1}^{N} U_{ik})^2$ to be order one. This is borne out by explicit calculations, see e.g. [13, 23, 30–32, 58–60, 69]. In other words, since the moduli couplings to axions are comparable to their couplings to the Standard Model particles, the string/M theory axiverse is in serious tension with observed limits on the amount of dark radiation. In special examples with low numbers of axions, one can see that it is possible to generate acceptably small amounts of dark radiation assuming certain couplings are small enough, for example, [58–62, 65–67]. But in general, this will be difficult to avoid.

2.3 String/M theory examples

2.3.1 Calabi-Yau Compactifications

In Calabi-Yau compactifications of superstring theories to four dimensions, The moduli and axion kinetic terms in the Lagrangian are derived from a function of the moduli fields called the Kahler potential, K, which, up to a coefficient is given by

$$K = -a \ln V_X \tag{2.33}$$

Here, V_X is the volume of the Calabi-Yau manifold (as a function of the moduli). This is a sum of terms with coefficients given by the triple intersection numbers d_{ijk}. The coefficient a takes different values, depending upon which string theory

one is considering. In the heterotic and Type IIA compactifications, the volume is given as a function of the Kahler moduli S_i as:

$$V_X = \sum_{i=1}^{n} d_{ijk} S_i S_j S_k \tag{2.34}$$

Clearly, in a completely generic case, with many non-zero entries in d_{ijk}, V_X is a sum of many terms and K_{ij} will not be diagonal. Hence, upon diagonalisation, when expanding around a particular vacuum state, the matrices C_{ij}, U_{ij} and the coefficients B_i and D_i will be quite general and we expect $N_{eff} \propto N$.

In the LARGE volume scenario of [13, 69], there is a modulus field with a vev much larger than that of the other moduli. In this case, the volume functional of the Calabi-Yau threefold is approximated by

$$V = s_1^{3/2} - s_2^{3/2} - \ldots - s_N^{3/2} \tag{2.35}$$

$$K = -2 \ln V \tag{2.36}$$

In the limit where the s_1 vev is larger than the other vevs, $s_1 \gg s_i$, the diagonalised Kahler metric is approximately

$$f_1 = K_{11} \approx \frac{3}{4 s_1^2}, \quad f_i = K_{ii} \approx \frac{3}{8 s_1^{3/2} s_i^{1/2}} \tag{2.37}$$

$$\partial_1 f_1 = -\frac{3}{2 s_1^3}, \quad \partial_i f_1 = 0, \quad \partial_1 f_i = -\frac{9}{16 s_1^{5/2} s_i^{1/2}}, \quad \partial_i f_i = -\frac{3}{16 s_1^{3/2} s_i^{3/2}} \tag{2.38}$$

For s_1, it turns out that $\Delta N_{eff} \propto N$. This can be seen as follows. The decay

widths to axions are

$$\Gamma(\hat{s}_1 \to \hat{t}_1\hat{t}_1) = \frac{1}{256\pi}\left(\frac{16}{3}\right)\frac{m^3}{m_{pl}^2} \tag{2.39}$$

$$\Gamma(\hat{s}_1 \to \hat{t}_{i\neq 1}\hat{t}_{i\neq 1}) = \frac{3}{256\pi}\frac{m^3}{m_{pl}^2} \tag{2.40}$$

$$\Gamma(\hat{s}_1 \to \text{axions}) = \frac{1}{256\pi}\left(\frac{16}{3} + 3(N-1)\right)\frac{m^3}{m_{pl}^2} \tag{2.41}$$

whilst the gauge boson channel gives

$$\Gamma(\hat{s}_1 \to \gamma\gamma) = \frac{1}{48\pi}\frac{\widetilde{a}_j^2\langle s_1^2\rangle}{\left(\sum_{i=1}^N \widetilde{a}_i\langle s_i\rangle\right)^2}\frac{m^3}{m_{pl}^2} \tag{2.42}$$

resulting in a dark radiation contribution of

$$\Delta N_{eff}(s_1) = \left(1 + \frac{9}{16}(N-1)\right)\frac{\left(\sum_{i=1}^N \widetilde{a}_i\langle s_i\rangle\right)^2}{\widetilde{a}_1^2\langle s_1^2\rangle} \tag{2.43}$$

This is interesting, because in LARGE volume models, the vev s_1 is expected to be much larger than the other vevs, hence one expects a suppression of ΔN_{eff} in this case, following our discussion in section two. Furthermore, s_1 is typically the lightest modulus in this scenario [69].

For completeness, for $s_{j\neq 1}$, the dark radiation density doesn't depend on N :

$$\Gamma(\hat{s}_{j\neq 1} \to \hat{t}_{j\neq 1}\hat{t}_{j\neq 1}) = \frac{1}{128\pi}\frac{\langle s_1\rangle^{3/2}}{\langle s_j\rangle^{3/2}}\frac{m^3}{m_{pl}^2} \tag{2.44}$$

$$\Gamma(\hat{s}_{j\neq 1} \to \hat{t}_{j\neq i}\hat{t}_{j\neq i}) = 0 \tag{2.45}$$

$$\Gamma(\hat{s}_{j\neq 1} \to \text{axions}) = \frac{1}{128\pi}\frac{\langle s_1\rangle^{3/2}}{\langle s_j\rangle^{3/2}}\frac{m^3}{m_{pl}^2} \tag{2.46}$$

gauge boson channel is

$$\Gamma(\hat{s}_{j\neq 1} \to \gamma\gamma) = \frac{1}{24\pi} \frac{\widetilde{a}_j^2 \langle s_j^{1/2} \rangle \langle s_1^{3/2} \rangle}{\left(\sum_{i=1}^N \widetilde{a}_i \langle s_i \rangle \right)^2} \frac{m^3}{m_{pl}^2} \tag{2.47}$$

So the total dark radiation density is proportional to

$$\Delta N_{eff}(s_{j\neq 1}) = \frac{3}{16} \frac{\left(\sum_{i=1}^N \widetilde{a}_i \langle s_i \rangle \right)^2}{\widetilde{a}_j^2 \langle s_j^2 \rangle} \tag{2.48}$$

2.3.2 Diagonal Kahler metrics

Clearly, from the above discussions, one can suppress dark radiation from moduli decays when the Kahler metric for the moduli fields is approximately diagonal. This will be the case when the Volume function is dominated by just one term only.

$$V_X = \prod_{i=1}^N S_i^{a_i}, \quad K = -3 \sum_{i=1}^N a_i \ln S_i \tag{2.49}$$

where a_i are microscopic parameters whose sum is a constant determined by the geometry of the extra dimensions. This is unity for the Calabi-Yau case and $\frac{7}{3}$ for G_2-manifolds. To demonstrate the suppression of N_{eff}, it is helpful to translate the effective supergravity Lagrangian into decay width coefficients. We review the calculation explicitly below.

The kinetics terms for moduli and axions are controlled by Kahler metric as following

$$\mathcal{L} = \frac{1}{2} K_{ij} \partial^\mu s^i \partial_\mu s^j + \frac{1}{2} K_{ij} \partial^\mu t^i \partial_\mu t^j \tag{2.50}$$

After canonically normalisation of moduli and axions, we can expand Kahler metric as a function of the moduli field. After taking the moduli mixing into

account, the result for the interaction Lagrangian is

$$\mathcal{L}_{\tilde{s}_k\tilde{t}_i\tilde{t}_i} = \frac{1}{2}\frac{\sum_{j=1}^{N}\frac{\partial K_{ii}^D}{\partial s_j}U_{jk}}{(K_{ii}^D)^{3/2}}\tilde{s}_k\partial^\mu\tilde{t}^i\partial_\mu\tilde{t}^j \tag{2.51}$$

where K^D is Kahler metric after diagonalisation. $\tilde{s}$, $\tilde{t}$ are canonically normalised fields after mixing. Straightforwardly, one can derive the decay width into axions as

$$\Gamma_{\text{axions}} = \frac{1}{32\pi}\sum_{i=1}^{N}\left(\sum_{j=1}^{N}\frac{1}{\sqrt{K_{ii}^D}}\frac{\partial \ln K_{ii}^D}{\partial s_j}U_{jk}\right)^2\frac{m_{X_k}^3}{M_{pl}^2} \tag{2.52}$$

For the gauge sector, the Lagrangian typically takes the form

$$\mathcal{L} = -\frac{1}{4}\left(\sum_{i=1}^{N}N_i z_i\right)F_{\mu\nu}F^{\mu\nu} \tag{2.53}$$

After canonically normalisation of moduli and gauge fields, we get the interaction terms between moduli and gauge fields.

$$\mathcal{L} = \frac{1}{4}\frac{1}{\left(\sum_{i=1}^{N}N_i\langle s_i\rangle\right)}\sum_{i=1}^{N}\frac{N_i U_{ik}}{\sqrt{K_{ii}^D}}\tilde{s}_k F_{\mu\nu}F^{\mu\nu} \tag{2.54}$$

Then the moduli decay width into gauge bosons/gauginos can be written as

$$\Gamma_{\text{gauge}} = \frac{N_G}{32\pi}\left(\sum_{i=1}^{N}\frac{\alpha}{\sqrt{K_{ii}^D}}N_i U_{ik}\right)^2\frac{m_{X_k}^3}{M_{pl}^2} \tag{2.55}$$

For matter sector, the generic interaction terms can be found from

$$\mathcal{L} = K_{\alpha\beta}D_\mu f^\alpha D^\mu f^\beta + K_{\alpha\beta}\tilde{f}^\alpha \not{D}\tilde{f}^\beta \tag{2.56}$$

Then, after normalisation of moduli field and fermions/sfermions fields, the inter-

action terms become

$$\mathcal{L} = \sum_{i=1}^{N} \frac{1}{\sqrt{K_{ii}^D}} \frac{\partial \ln K_{\alpha\alpha}^D}{\partial s_i} U_{ik} \tilde{s}_k \left(D_\mu f^\alpha D^\mu f^\alpha + \tilde{f}^\alpha \not{D} \tilde{f}^\alpha \right) \tag{2.57}$$

Therefore, the decay width into fermion can be written as

$$\Gamma_{\text{fermion}} \propto \left(\sum_{i=1}^{N} \frac{1}{\sqrt{K_{ii}^D}} \frac{\partial \ln K_{\alpha\alpha}^D}{\partial s_i} U_{ik} \right)^2 \frac{m_{X_k}^3}{M_{pl}^2} \tag{2.58}$$

To summarise, the decay width coefficients are given as follow:

$$\begin{aligned} C_{ij} &= \frac{1}{\sqrt{K_{ii}^D}} \frac{\partial \ln K_{ii}^D}{\partial s_j} \\ B_i &= \frac{\alpha}{\sqrt{K_{ii}^D}} N_i \\ D_i &= \frac{1}{\sqrt{K_{ii}^D}} \frac{\partial \ln K_{\alpha\alpha}^D}{\partial s_i} \end{aligned} \tag{2.59}$$

where K_{ij}^D is the diagonal Kahler metric.

From (2.49), it is trivial to show that the coefficients are diagonal when the volume function is dominated by a single term:

$$C_{ij} = C_i \delta_{ij} \tag{2.60}$$

Following the previous analysis, this simple relation implies that ΔN_{eff} becomes independent of N on average.

$$\langle \Delta N_{eff} \rangle \propto \frac{\langle C \rangle^2}{n_G \langle B \rangle^2 + n_f \langle D \rangle^2} \tag{2.61}$$

where the orthogonality of rotation matrix, $(\sum_{i=1}^{N} U_{ik}^2) = 1$, has been used.

The physical reason for this behaviour is that this particular volume form

forces each modulus to decay only into its axionic partner. If we assume further that this basis is already physical, i.e. there is no further mixing between moduli or axions, it becomes clear that dark radiation, regardless of N, consists of only one species of axion which is the partner of the last modulus to decay.

The moduli mixing matrix can also play a role in suppressing dark radiation. Again, though non-generic, this occurs when there is a relation between the moduli mass matrix and the eigenvalues of the Kahler metric:

$$\sqrt{K^D_{ii}} \propto U_{ij} \tag{2.62}$$

The above relation is equivalent to

$$\frac{1}{C_i} \propto U_{ik},\ \frac{1}{B_i} \propto U_{ik},\ \frac{1}{D_i} \propto U_{ik} \tag{2.63}$$

In this case, the correlation becomes

$$\langle \Delta N_{eff} \rangle \propto \frac{N\langle C \rangle^2}{n_G N^2 \langle B \rangle^2 + n_f N^2 \langle D \rangle^2} \propto \frac{1}{N} \tag{2.64}$$

Therefore, under these very special circumstances, dark radiation can actually be suppressed by the number of axions on average. This counter-intuitive result is merely the effect of increasing N-dependence of the moduli to visible sector couplings so that dark radiation is dominated by standard model radiation (neutrinos). Most likely, this is merely a curious observation rather than a realistic case.

Mass matrix in G_2 compactified M-theory

In this subsection, we put together some of these results in a concrete setting where the moduli mass matrix is known, namely G_2-compactified M theory. Again, we are assuming that K is dominated by a single term:

$$K = -3 \ln \left(\prod_{i=1}^{N} s_i^{a_i} \right) \tag{2.65}$$

where $\sum_{i=1}^{N} a_i = \frac{7}{3}$. From above, N_{eff} becomes independent of the number of axions in this model. However, regardless of this advantage, one could easily find that the typical value of N_{eff}, although independent of N, is actually too large in practice e.g. $\Delta N_{eff} \sim 10$. We would therefore like to investigate the possibility of further suppressing dark radiation in this setup.

We briefly recall some details of moduli stabilisation. It has been shown in [31] that with a hidden sector with two gauge groups where first group is sQCD with 1 flavour of quarks and second group is pure glue sQCD leads to dS vacua. The superpotential is written as

$$W = A_1 \phi^a e^{ib_1 \sum_i^N N_i S_i} + A_2 e^{ib_2 \sum_i^N N_i S_i} \tag{2.66}$$

where ϕ is the meson superfield in the hidden sector. With the superpotential and Kahler potential being specified, it is straightforward yet tedious to work out

the mass mixing matrix resulting from moduli stabilisation [23, 30].

$$
\begin{aligned}
U_{kj} = \sqrt{\frac{a_{j+1}}{(\sum_{i=1}^{j} a_i)(\sum_{i=1}^{j+1} a_i)}}\sqrt{a_k}, \quad , \quad k \leq j \\
U_{kj} = -\sqrt{\frac{\sum_{i=1}^{j} a_i}{\sum_{i=1}^{j+1} a_i}} \quad , \quad k = j+1 \\
U_{kN} = \sqrt{\frac{3a_k}{7}}
\end{aligned}
\tag{2.67}
$$

where $i = 1 \ldots N-1$ are the degenerate light moduli and $i = N$ is heavy modulus. Notice that except $k = j+1$, $U_{kj} \propto \sqrt{a_k} \propto \sqrt{K_k}$. Therefore, we the element $U_{j+1,j}$ will be suppressed if it turned out that:

$$
\sum_{i=1}^{j} a_i \ll a_{j+1} \tag{2.68}
$$

As a result, one would expect $\frac{1}{N}$ suppression on dark radiation under this condition.

The modulus decay width can be calculated from [23]

$$
\begin{aligned}
\Gamma_{X_j} &= D_{X_j} \frac{m_{X_j}^3}{M_{Pl}^2} \\
D_{X_j} &= \alpha \left(\sum_{k=1}^{N} \frac{U_{kj}^2}{a_k} \right) + \beta \left(\sum_{k=1}^{N} \frac{U_{kj}}{\sqrt{a_k}} \right)^2
\end{aligned}
\tag{2.69}
$$

where α and β are index-independent parameters dependent on the microscopic details of the G_2 manifold. The first term represents the decay width into axions where the latter represents decay width into visible particles. From (2.67) and (2.69) it is trivial to see that total decay width of j^{th} modulus and corresponding

dark radiation are controlled by

$$\Gamma_j \propto \frac{\sum_{i=1}^{j} a_i}{a_{j+1}} \tag{2.70}$$

$$\Delta N_{eff}(X_j) \propto \frac{j a_{j+1}^2 + (\sum_{i=1}^{j} a_i)^2}{(j a_{j+1} - \sum_{i=1}^{j} a_i)^2} \tag{2.71}$$

Applying (2.68), we clearly see that $\Delta N_{eff}(X_j) \propto \frac{1}{j}$ and Γ_j becomes smallest. This is essential to the model because it guarantees that the last decay modulus exhibits $\frac{1}{N}$ behaviour. For practical purpose, only $j = N - 1$ in condition (2.68) will be assumed.

Next, we will explicitly show correlations between the number of axions and N_{eff}. Instead of scanning the N parameters a_i space, we will give systematic examples of simple configurations of the a_i which work:

The first example is when n of the a_i are large and the rest small:

$$a_i = \{\underbrace{\epsilon\bar{a}, \ldots, \epsilon\bar{a}}_{N-n}, \underbrace{\frac{7}{3n} - \frac{\epsilon\bar{a}(N-n)}{n}, \ldots, \frac{7}{3n} - \frac{\epsilon\bar{a}(N-n)}{n}}_{n}\} \tag{2.72}$$

The second is a geometric sequence of a_is,

$$a = \{a_0, a_0, a_0 r, a_0 r^2, \ldots, a_0 r^{N-2}\} \tag{2.73}$$

Though these can be viewed as toy models at best, they both illustrate that, in principle, the amount of dark radiation can actually *decrease* as one increases the number of axions. This is illustrated in the two figures.

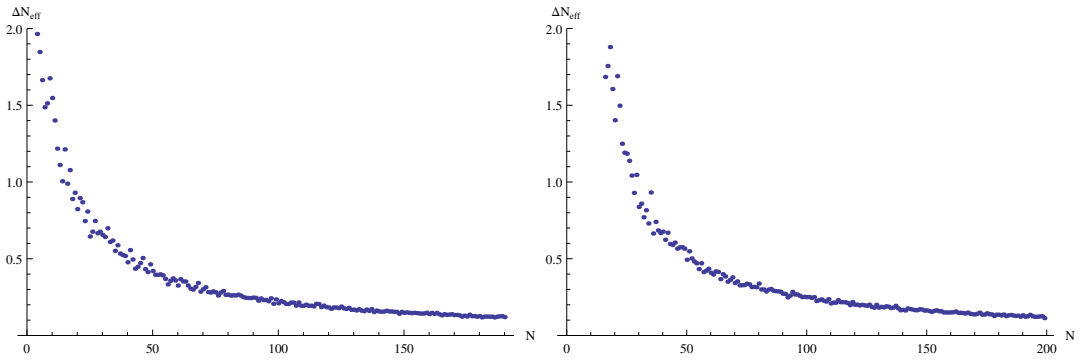

(a) (b)

Figure 2.1: Left: Result from geometric sequence configurations showing ΔN_{eff} as a function of N, where $r = 2$. Right: Result from double moduli dominated configurations showing ΔN_{eff} as a function of N, where $\epsilon N = 0.1$

2.4 Conclusions and Outlook

ΔN_{eff} is a very powerful probe of light degrees of freedom in the hidden sector and, somewhat surprisingly, has been constrained to be quite small, consistent with zero. The Axiverse induced Dark Radiation Problem arises from the plethora of light degrees of freedom that can be present in string/M theory compactifications to four dimensions. Though we focused on the axions, similar conclusions can be drawn from hidden photons and other light particles in the hidden sector. We pointed out several possible mechanisms via which this problem could be avoided: a) a relatively large modulus vev as in the LARGE volume scenario; b) alignment between the axion kinetic and mass mixing matrices so that the last modulus to decay does so predominantly into its axionic partner. It would be very interesting to explore these mechanisms in more detail in various specific models. One potential problem with the large vev solution in practice is that the large vev corresponds to a weak Standard Model coupling. In general, it might be difficult to make the vev large enough without making the Standard Model coupling too small.

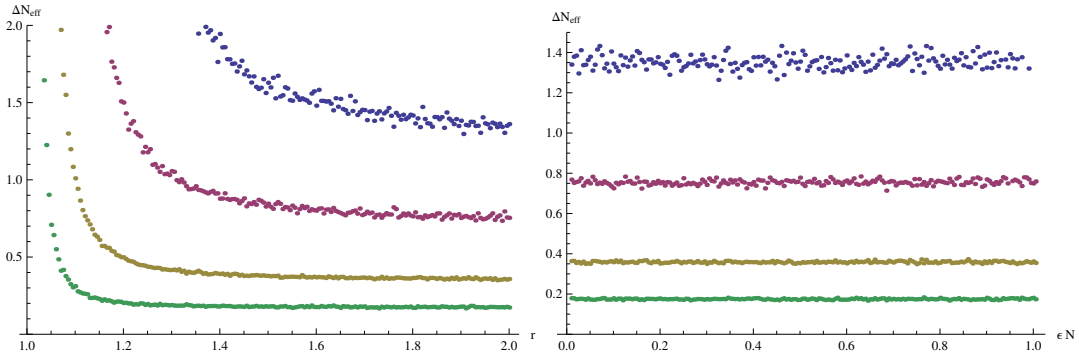

(a) (b)

Figure 2.2: Left: Result from geometric sequence configurations showing ΔN_{eff} as a function of r, where points in blue, red, yellow, green are $N = 30, 50, 100, 200$ respectively. Right: Result from double moduli dominated configurations showing ΔN_{eff} as a function of ϵN, where points in blue, red, yellow, green are $N = 30, 50, 100, 200$ respectively

Chapter 3

Particle Physics from M theory inspired models

3.1 Introduction

Results over the past decade or so have shown that the simple combination of supersymmetry breaking moduli stabilisation and string/M theory can in fact be a very useful guide to constructing models [12,13,31,32,70]. Namely, the progress in understanding supersymmetry breaking and moduli stabilisation in string/M theory has been shown to lead to effective models with distinctive features and very few parameters.

One is thus led to consider supersymmetric grand unified theories (GUTs) based on simple groups, such as $SU(5)$ which explain the fermion quantum numbers and unify the three Standard Model forces, in the string/M theory context. In doing so, however, we have to face the basic problem of GUTs – the Higgs doublet-triplet splitting problem: the Standard Model Higgs doublet is unified into a GUT multiplet containing colour triplets which can mediate proton decay

too quickly. In many models, including those originating in string/M theory, this problem is often solved by making the colour-triplets very massive [71–73], something often achieved with a discrete symmetry whose effective action on the triplets is different from that on the doublets.

In this chapter, we will extend the scope of the M theory approach from the previously considered $SU(5)$/MSSM case arising from M theory on G_2 manifolds [32, 74] to $SO(10)$, where an entire fermion family Q, u^c, d^c, L, e^c, N, including a charge conjugated right-handed neutrino N, is unified within a single **16** representation denoted $\mathbf{16}^m$. In particular we focus on the Higgs doublet-triplet splitting problem, whose solution turns out to be necessarily quite different in the $SO(10)$ case, leading to distinct phenomenological constraints and predictions. We first review some basic ideas and results from M theory, followed by review on discrete symmetry and μ problem, then we will review $SU(5)$ models as an example before moving on to a discussion of the new $SO(10)$ case.

3.1.1 M theory on G_2 manifolds

In this section, we provide a review on the phenomenology of the low energy limit of compactified M theories on a G_2 manifold. The in-depth details can be found in [30–32]. It has been shown that M theory compactifed on a G_2 manifold gives rise to a 4D theory with $\mathcal{N} = 1$ supersymmetry. The gauge fields and the chiral fermions arise from different types of singularities on the G_2 manifolds [38]. A G_2 manifold with fluxes would generate a large mass scale and therefore it is not phenomenologically interesting. Instead, we assume that only non-perturbative effect plays a role in moduli stabilisation. We will consider G_2 manifolds which have 2 non-abelian asymtotically free gauge groups, $SU(Q) \times SU(P+1)$ where a pair of vector like quarks is charged under $SU(P+1)$. At energies lower than these gauge

groups confinement scales, the superpotential is generated non-perturbatively as

$$W = M_{Pl}^3 \left(C_1 P \phi^{2/P} e^{ib_1 f_1} + C_2 Q e^{ib_2 f_2} \right), \; b_1 = \frac{2\pi}{P}, \; b_2 = \frac{2\pi}{Q} \tag{3.1}$$

where ϕ is the effective meson field coming from a pair of vector like quarks. C_1, C_2 are normalisation constants which are calculable for a given G_2 manifold. f_1 and f_2 are gauge kinetic functions of the two hidden sectors which are generically different from each others. To study the vacua semi-analytically, we assume

$$f_1 = f_2 = f_{hid} = \sum_{i=1}^{N} N^i (t_i + i s_i) \tag{3.2}$$

where s_i are the N geometric moduli from the metric of G_2 manifold, a_i are the axions as zero modes of the 3-form fields, and N^i are integers determined by the homology class of the hidden sector 3-cycles.

The supergravity potential is fully determined when the superpotential and the Kahler potential are given. However, it is generically difficult to compute the matter Kahler potential from first principle. Due to the fact that chiral supermultiplets are localised in 3-dimensional subspaces, we assume that the Kahler potential takes the canonical form

$$\frac{K}{M_{Pl}^2} = -3 \ln(4\pi^{1/3} V_7) + \overline{\phi}\phi \tag{3.3}$$

where V_7 is the volume of the G_2 manifold in units of the eleven-dimensional Planck length. The volume is parametrised by the moduli as $V_7 = \prod_{i=1}^{N} s_i^{a_i}$ where a_i are positive rational numbers constrained by $\sum_{i=1}^{N} a_i = 7/3$.

The values of the moduli at the minima are given by the set of constants determining the potential $\{a_i, N^i, C_1, C_2, P, Q, N\}$ which are calculable for a given

G_2 manifold consistent with our assumptions. It was shown in [30] that all moduli are stabilised with a vev $\langle s_i \rangle \simeq \mathcal{O}(0.1) M_{Pl}$ leading to supersymmetry breaking and a small cosmological constant. Note that the F term of the meson field is much greater than those of moduli fields, $F_\phi \simeq \mathcal{O}(0.01) m_{3/2} M_{Pl}$ where $m_{3/2}$ is the gravitino mass characterising susy breaking scale.

The observable sector gauge theory lives in a three-manifold different from the one supporting the hidden sector. The conical singularities on the observable three-manifold support chiral matter fields. The full low energy supergravity theory of the visible and hidden sectors is defined by the following:

$$\frac{K}{M_{Pl}^2} = \left(-3\ln(4\pi^{1/3}V_7) + \overline{\phi}\phi\right) + \widetilde{K}_{\overline{\alpha}\beta}(s_i)\overline{\Phi}^{\overline{\alpha}}\Phi^\beta + (Z(s_i)H_u H_d + h.c.) + \ldots \quad (3.4)$$

$$W = M_{Pl}^3\left(C_1 P\phi^{2/P} e^{ib_1 f_1} + C_2 Q e^{ib_2 f_2}\right) + Y'_{\alpha\beta\gamma}\Phi^\alpha\Phi^\beta\Phi^\gamma \quad (3.5)$$

$$f_1 = f_2 = f_{hid} = \sum_{i=1}^{N} N^i(t_i + is_i),\ Im(f^0_{vis}) = \sum_{i=1}^{N} N^i_{vis} s_i \quad (3.6)$$

The visible sector is thus characterised by the Kahler metric $\widetilde{K}_{\overline{\alpha}\beta}$ and un-normalised Yukawa couplings $Y'_{\alpha\beta\gamma}$ of the visible sector chiral matter fields Φ^α and the tree-level gauge kinetic function f^0_{vis} of the visible sector gauge fields. The un-normalised Yukawa couplings in these vacua arise from membrane instantons which connect singulartities where chiral superfields are supported.

$$Y'_{\alpha\beta\gamma} = C_{\alpha\beta\gamma} e^{i2\pi\sum_i l_i^{\alpha\beta\gamma}(t_i + is_i)} \quad (3.7)$$

where $C_{\alpha\beta\gamma}$ is an $\mathcal{O}(1)$ constant and $l_i^{\alpha\beta\gamma}$ are integers characterising the 3-cycle encapsulating the three singularities supporting the chiral multiplets $\Phi^\alpha, \Phi^\beta, \Phi^\gamma$.

Given the effective supergravity lagrangian, one can evaluate the soft terms from the vevs of the scalar and auxiliary fields of the moduli. The order parameter

for the breaking is given by the gravitino mass

$$m_{3/2} = e^{\frac{K}{2M_{Pl}}} \frac{|W|}{M_{Pl}^2} \tag{3.8}$$

which is found to naturally lies between 10 - 100 TeV. The gravitino mass sets the scale of all scalar in supergravity. The soft scalar masses [75] (after normalisation of the visible Kahler potential) can be expressed as

$$m_{\overline{\alpha}\beta}^2 = (m_{3/2}^2 + V_0)\delta_{\overline{\alpha}\beta} - \mathcal{U}^\dagger \Gamma_{\overline{\alpha}\beta} \mathcal{U} \tag{3.9}$$

$$\Gamma_{\overline{\alpha}\beta} \equiv e^{\hat{K}} F^{\overline{m}} \left(\partial_{\overline{m}} \partial_n \widetilde{K}_{\overline{\alpha}\beta} - \partial_{\overline{m}} \widetilde{K}_{\overline{\alpha}\gamma} \widetilde{K}^{\gamma\overline{\delta}} \partial_n \widetilde{K}_{\overline{\delta}\beta} \right) F^n \tag{3.10}$$

In order to calculate the non-diagonal and non-universal parts, we need to know the moduli and meson dependence. However, it is known to be difficult to compute in a generic string and M theory vacua. We assume here that the non-diagonal and non-universal parts depend on only F-term of moduli and meson fields. From $F_i << F_\phi$, we get

$$m_{\overline{\alpha}\beta}^2 \approx m_{3/2}^2 \delta_{\overline{\alpha}\beta} \tag{3.11}$$

This result implies that the flavor changing neutral currents will be suppressed. The calculation of the un-normalised trilinear couplings is simplified by the same assumptions and given by

$$A'_{\alpha\beta\gamma} = \frac{\hat{W}*}{|\hat{W}|} e^{\hat{K}} F^\phi \hat{K}_\phi Y'_{\alpha\beta\gamma} \tag{3.12}$$

The normalised couplings can be obtained

$$A_{\alpha\beta\gamma} \approx \mathcal{O}(1) m_{3/2} Y_{\alpha\beta\gamma} \tag{3.13}$$

Notice that in our framework, the scalar soft masses and trilinear terms are of order $m_{3/2}$.

The computation of gaugino masses does not depend on the matter Kahler potential. In G_2 vacua, the tree-level contribution is suppressed therefore other contributions such as anomaly mediation and threshold effects can be equally important. It has been shown in [30] that at the unification scale the gaugino masses are expected to be

$$m^a_{1/2} = \mathcal{O}(100 \text{ GeV}) \tag{3.14}$$

Note that the gaugino masses are not universal due to contribution from the anomaly mediation.

3.1.2 Discrete symmetry and Wilson line

One of the main problems of GUT theories is the fast proton decay mediated by colour triplet partners of Higgs doublets. To prevent a significant decay rate, the colour triplets must be either very massive (often of order GUT scale) or completely decoupled from the standard model sector. For most string theories, the splitting/decoupling can be accomplished by a Wilson line in the higher dimensional theory, but in M theory, this is not possible since matter only exists in four dimensions. It was then noticed by Witten [74] that the presence of a geometric discrete symmetry of the G_2 manifolds whose action is enhanced by Wilson line phases leads to a symmetry that does not commute with the GUT gauge group. Therefore, this allows different components of the GUT multiplet to have different discrete charges and hence preventing proton decay. Here I will review the mechanism in SU(5) GUT theories studied in [45] before proceeding to SO(10)

GUT theories in later sections.

In M-theory compactified on a hidden manifold X with G_2 holonomy, gauge fields are localised on a 3 dimension submanifold K, whereas the chiral multiplets are localised on points in K where a conical singularity is developed. To break the GUT symmetry, we assume that K is not simply-connected. Since the fundamental group of K is non-vanishing, there exists a non-trivial gauge field configurations, i.e., a Wilson line. The GUT group is broken down into the subgroup that commutes with Wilson lines. If the survival subgroup has n U(1) factors then a Wilson line can be expressed as

$$\mathcal{W} = \exp\left(\frac{i2\pi}{N}\sum_{i}^{n} a_i Q_i\right) = \sum_{m=0}^{\infty}\frac{1}{m!}\left(\frac{i2\pi}{N}\sum_{i=1}^{n} a_i Q_i\right)^m \quad , \tag{3.15}$$

where Q_i are the generators of the U(1) factors, a_i are coefficients of the linear combination that are only constrained by $\mathcal{W}^N = 1$.

If K admits a discrete symmetry of the geometry isomorphic to the fundamental group which we assume to be $\mathbf{Z_N}$ symmetry for simplicity, the discrete symmetry action and the Wilson line charges would mix leading to a discrete symmetry that does not commute with the GUT group. This means we have non-GUT preserving selection rules, which will constraint our Lagrangian below the GUT scale.

To illustrate how Witten's proposal leads to preventing proton decay, let's consider the case of $SU(5)$ as shown in [45]. We assume the following: $\overline{\mathbf{5}}^w$ is the multiplet containing H_d and $\overline{D}$ and is localised along the Wilson line; $\mathbf{5}^h$ is the multiplet containing H_u; $\overline{\mathbf{5}}^m$ and $\mathbf{10}^m$ are the matter multiplets. Then the

transformation rules for these multiplets under $\mathbf{Z_N}$ are:

$$\begin{aligned}
\overline{\mathbf{5}}^w &\to \eta^\omega \left(\eta^\delta H_d^w \oplus \eta^\gamma \overline{D}^w\right), \\
\mathbf{5}^h &\to \eta^\chi \mathbf{5}^h, \\
\overline{\mathbf{5}}^m &\to \eta^\tau \overline{\mathbf{5}}^m, \\
\mathbf{10}^m &\to \eta^\sigma \mathbf{10}^m,
\end{aligned} \tag{3.16}$$

where $\eta \equiv e^{2\pi i/N}$, $2\delta + 3\gamma = 0 \mod N$. By requiring that Yukawa couplings, Majorana neutrino masses, and colour-triplet masses must be present, we obtain constraints on the charges as can be seen in Table 3.1 where we chose $\omega = 0$. One can solve these by writing all angles in terms of σ.

$$\begin{aligned}
\chi &= -\gamma = -2\sigma \mod N \\
\delta &= -3\sigma + N/2 \mod N \\
\tau &= 2\sigma + N/2 \mod N
\end{aligned} \tag{3.17}$$

The μ term and other proton decay operators must also be forbidden. The constraints are shown in Table 3.2. It is then trivial to see that all of the constraints are satisfied with a Z_4 symmetry. For example, $N = 4$, $\sigma = 1$.

Coupling		Constraint
Up-type Yukawas	$H_u^h \mathbf{10}^m \mathbf{10}^m$	$2\sigma + \chi = 0 \mod N$
Down-type Yukawas	$H_d^w \mathbf{10}^m \overline{\mathbf{5}}^m$	$\sigma + \tau + \delta = 0 \mod N$
Majorana Masses of neutrinos	$H_u^h H_u^h \overline{\mathbf{5}}^m \overline{\mathbf{5}}^m$	$2\chi + 2\tau = 0 \mod N$
Colour-triplet masses	$\overline{D}^w D^h$	$\chi + \gamma = 0 \mod N$

Table 3.1: Couplings and charges for $SU(5)$ operators.

Coupling		Constraint
μ term	$H_d^w H_u^h$	$-5\sigma + N/2 \neq 0 \bmod N$
Dimension 5 proton decay	$\mathbf{10}^m\mathbf{10}^m\mathbf{10}^m\overline{\mathbf{5}}^m$	$5\sigma - N/2 \neq 0 \bmod N$
Dimension 3 R-parity violation	$\mathbf{5}_H\overline{\mathbf{5}}^m$	$N/2 \neq 0 \bmod N$
Dimension 4 R-parity violation	$\mathbf{10}^m\overline{\mathbf{5}}^m\overline{\mathbf{5}}^m$	$5\sigma \neq 0 \bmod N$

Table 3.2: Couplings and charges for $SU(5)$ operators.

3.1.3 Effective μ-terms and trilinear couplings

In an essence of the doublet-triplet splitting mechanism from the discrete symmetry arising from earlier arguments, the Higgs doublets mass parameter, μ must vanish at the GUT scale. However, the limit on the Higgsinos mass constrains $\mu \geq \mathcal{O}(100)$ GeV. The discrete symmetry must therefore be broken. In M Theory compactified on a G_2 manifold without fluxes there is a natural way of generating effective μ terms. An effective μ-term of order TeV scale can be generated by moduli vev from interactions in the Kahler potential, the mechanism which is similar to Giudice-Masiero mechanism [44].

To see how the above considerations lead to a natural $\mathcal{O}(1$ TeV$)$ μ term consider the Kahler potential interaction

$$K \supset \frac{s}{m_{Pl}} X\overline{X} + \text{h.c.}\ , \tag{3.18}$$

here we take the coefficient to be or order one, and s symbolically represents a modulus field, and X a chiral supermultiplet in some gauge irrep, with $\overline{X}$ another chiral supermultiplet in the charge conjugated irrep. As moduli arise from zero modes of the Lichnerowicz equation, they are naturally charged under the discrete symmetry. Since there are many of them, the above coupling is generally allowed even if $X\overline{X}$ is forbidden by the same discrete symmetry.

As a consequence of the moduli stabilisation and associated vevs, an effective μ

parameter for the X field will be generated. This effective parameter appearing in the superpotential is derived from the usual supergravity mass formulae [75] [76] when taking the flat – *global SUSY* – limit of supergravity.

In the end one finds that the effective superpotential μ term is given by

$$\mu_X = \langle m_{3/2} K_{X\overline{X}} - F^{\overline{\kappa}} K_{X\overline{X}\kappa} \rangle \ , \tag{3.19}$$

which leads to

$$\mu_X = \frac{\langle s \rangle}{m_{Pl}} m_{3/2} + \frac{\langle F_s \rangle}{m_{Pl}} \ , \tag{3.20}$$

and since $F_s \ll m_{3/2}\langle s \rangle$ the moduli vev dominates. One finds

$$\mu_X \sim 0.1 m_{3/2} \ , \tag{3.21}$$

and since $m_{3/2} \sim \mathcal{O}(10 \text{ TeV})$, we have $\mu_X \simeq \mathcal{O}(1 \text{ TeV})$. Notice that this analysis is valid for all vector-like pairs $X\overline{X}$. This means that if one adds extra vector-like states to the model, beyond the MSSM spectrum, one has to worry about possible mixings and LHC-reachable extra fermionic matter. This will be studied below when we construct the SO(10) model.

Similar to the above procedure to generate μ parameters, our framework can generate effective trilinear terms in the superpotential. They will mediate proton decay but also provide a LSP decay channel, since they can be R-parity violating. These interactions play an important role for the low-energy model, and have to be studied in detail.

Trilinear interactions are generated in the same way as the effective μ terms

dsicussed above. Consider the Kahler potential contribution

$$K \supset \frac{s}{m_{pl}^2} XYZ + \text{h.c.} \ , \tag{3.22}$$

where s does not have to be the same moduli as above, and X, Y, and Z are chiral supermultiplets. As one can see, these interactions are more suppressed than the effective μ-terms studied before, they will, however, still appear as effective trilinear couplings in the superpotential as

$$W_{eff} \supset \frac{(\langle s \rangle m_{3/2} + F_s)}{m_{pl}^2} m_{3/2} XYZ \ , \tag{3.23}$$

Again, since $F_s \ll \langle s \rangle m_{3/2}$, the F-term contribution is sub-leading and we can estimate the order of magnitude of the effective coupling. This turns out to be small

$$\frac{\langle s \rangle}{m_{pl}^2} m_{3/2} \to 0.1 \frac{m_{3/2}}{m_{Pl}} \sim 10^{-14} \ , \tag{3.24}$$

but it will have a deep impact on the LSP lifetime, as it will be discussed below.

We also note that in principle these cannot be big enough to generate realistic Yukawa couplings. One is then led to expect the Yukawa couplings to be generated by tree-level interactions as discussed above.

3.2 $SO(10)$

Following the review, we now turn to the M theory approach to $SO(10)$, where a novel solution to the doublet-triplet splitting problem seems to be required. Since the Wilson line is in the adjoint representation, it can break $SO(10)$ to $SU(3) \times SU(2) \times U(1)_Y \times U(1)$ and the Wilson line itself is a combination of $U(1)_Y$ and the additional $U(1)$. If we consider a fundamental of $SO(10)$ localised

along a Wilson line, then its transformation properties under the $\mathbf{Z_N}$ symmetry are

$$\mathbf{10}^w \to \eta^\omega \left(\eta^{-\alpha} H_d^w \oplus \eta^\beta \overline{D}^w \oplus \eta^\alpha H_u^w \oplus \eta^{-\beta} D^w\right). \tag{3.25}$$

In minimal $SO(10)$ the μ-term arises from a term in the superpotential of the form

$$W \supset \mu \mathbf{10}^w \mathbf{10}^w = \mu \left(H_u^w H_d^w + D^w \overline{D}^w\right), \tag{3.26}$$

The discrete symmetry will forbid this term in a general model. As in the $SU(5)$ case, once the symmetry is broken by moduli vevs, the term will be generated in the Kähler potential via the Giudice-Masiero mechanism. This will give a μ-term at the TeV scale, which, in $SO(10)$ also generates a similar mass for the triplet D.

We can add extra **10** multiplets and forbid some couplings between the different members of the various **10** multiplets. Consider one additional **10**, denoted $\mathbf{10}^h$ without Wilson line phases: $\mathbf{10}^h \to \eta^\xi \mathbf{10}^h$. We have eight possible gauge invariant couplings with a $\mathbf{10}^w$ and $\mathbf{10}^h$ that can be written in matrix form as

$$W \supset \mathbf{H}_d^T \cdot \mu_H \cdot \mathbf{H}_u + \overline{\mathbf{D}}^T \cdot M_D \cdot \mathbf{D}, \tag{3.27}$$

where μ_H and M_D are two 2×2 superpotential mass parameters matrices, $\mathbf{H}_{u,d}^T = \left(H_{u,d}^w, H_{u,d}^h\right)$, $\overline{\mathbf{D}}^T = \left(\overline{D}^w, \overline{D}^h\right)$, and $\mathbf{D}^T = \left(D^w, D^h\right)$. The entries of the matrices are non-vanishing depending on which of the following discrete charge combina-

tions are zero (mod N)

$$\begin{aligned} D^w\overline{D}^w,\ H_u^w H_d^w &:\ 2\omega, \\ D^h\overline{D}^h,\ H_u^h H_d^h &:\ 2\xi, \\ H_u^w H_d^h &:\ \alpha+\omega+\xi, \\ H_u^h H_d^w &:\ -\alpha+\omega+\xi, \\ D^w\overline{D}^h &:\ -\beta+\omega+\xi, \\ D^h\overline{D}^w &:\ \beta+\omega+\xi. \end{aligned} \tag{3.28}$$

The doublet-triplet splitting solution would be for μ_H to have only one zero eigenvalue, with M_D having all non-zero eigenvalues, i.e., all except a pair of Higgs doublet are massive. One finds that there is no choice of constraints within a Z_N symmetry from Eq. (3.28) that accomplishes this. It was shown that a possibility of adding more **10** multiplets does not work as well. Therefore, we shall only consider a single light $\mathbf{10}^w$, without any extra **10** multiplets at low energies.

Assuming a single light $\mathbf{10}^w$, it is possible to use the discrete symmetry to forbid certain couplings, namely to *decouple* D^w *and* $\overline{D}^w$ *from matter*. Such couplings arise from the operator $\mathbf{10}^w\mathbf{16}^m\mathbf{16}^m$, with $\mathbf{16}^m$ denoting the three $SO(10)$ multiplets, each containing a SM family plus right handed neutrino N. If $\mathbf{16}^m$ transforms as $\eta^\kappa\mathbf{16}^m$, the couplings and charge constraints are in Table 3.3, where we allow for up-type quark Yukawa couplings together with couplings to the right-handed neutrinos,

$$y_u^{ij} H_u^w \mathbf{16}_i^m \mathbf{16}_j^m \equiv y_u^{ij} H_u^w (Q_i u_j^c + L_i N_j + i \leftrightarrow j), \tag{3.29}$$

and similarly for down-type quarks and charged leptons. Explicit examples real-

ising these conditions will be given later.

Table 3.3: Couplings and charges for $SO(10)$ operators.

Coupling	Constraint
$H_u^w \mathbf{16}^m \mathbf{16}^m$	$2\kappa + \alpha + \omega = 0 \bmod N$
$H_d^w \mathbf{16}^m \mathbf{16}^m$	$2\kappa - \alpha + \omega = 0 \bmod N$
$D^w \mathbf{16}^m \mathbf{16}^m$	$2\kappa - \beta + \omega \neq 0 \bmod N$
$\overline{D}^w \mathbf{16}^m \mathbf{16}^m$	$2\kappa + \beta + \omega \neq 0 \bmod N$

The suppression of colour triplet couplings to matter was previously considered by Dvali in [77] and also [78–80] from a bottom-up perspective.

Next we consider the breaking of the discrete symmetry via the moduli vevs as discussed above, leading to proton decay. For proton decay, the relevant operators can be generated in the Kähler potential, schematically, writing $D = D^w$,

$$\begin{aligned} K \supset & \tfrac{s}{m_{pl}^2} DQQ + \tfrac{s}{m_{pl}^2} De^c u^c + \tfrac{s}{m_{pl}^2} DNd^c + \\ & + \tfrac{s}{m_{pl}^2} \overline{D} d^c u^c + \tfrac{s}{m_{pl}^2} \overline{D} QL. \end{aligned} \tag{3.30}$$

Just like the μ-term, the effective superpotential may be calculated from supergravity to be

$$\begin{aligned} W_{eff} \supset & \lambda DQQ + \lambda De^c u^c + \lambda DNd^c + \\ & + \lambda \overline{D} d^c u^c + \lambda \overline{D} QL, \end{aligned} \tag{3.31}$$

where

$$\lambda \approx \frac{1}{m_{pl}^2} \left(\langle s \rangle m_{3/2} + \langle F_s \rangle \right) \sim 10^{-14}. \tag{3.32}$$

Notice that unlike the case of SU(5), there is no SO(10) invariant bilinear term $\kappa L H_u$ whose presence would lead to fast proton decay. We estimate the scalar

triplet induced proton decay rate to be

$$\Gamma_p \approx \frac{|\lambda^2|^2}{16\pi^2}\frac{m_p^5}{m_D^4}. \tag{3.33}$$

Generically, the mass of the colour triplets is of the same order as μ, i.e., $m_D \sim 10^3$ GeV, so the proton lifetime is

$$\tau_p = \Gamma_p^{-1} \sim 10^{38} \text{ yrs}, \tag{3.34}$$

which exceeds the current experimental limit.

Now consider the D triplet decay rate:

$$\Gamma_D \sim \lambda^2 m_D \sim (0.1 \text{ sec})^{-1}. \tag{3.35}$$

The associated lifetime of 0.1 sec is (just) short enough to be consistent with BBN constraint. They will also give interesting collider signatures due to their long-lived nature.

3.2.1 Vector-like Family

Gauge coupling unification is in general spoiled by light colour triplets, unless they are also accompanied by additional light doublet states. In the present framework, the only way we know of to circumvent this issue is the presence of light additional states which complete the triplets into complete GUT multiplets. Happily, this can also be achieved by use of the discrete symmetry. First we introduce a vector-like pair of **16**'s, labelled as $\mathbf{16}_X + \overline{\mathbf{16}}_X$. Next a GUT-scale mass is given to their colour triplet components $d^c_X, \overline{d^c}_X$ whilst keeping the remaining particles light. Suitable charges under the discrete symmetry can forbid the appropriate mass

terms and the large mass can arise from membrane instantons if the $\mathbf{16}_X$ and $\overline{\mathbf{16}}_X$ are close by on the G_2 manifold [71].

We take $\mathbf{16}_X$ to be localised along a Wilson line, and find that it transforms under the discrete symmetry as

$$\begin{aligned}\mathbf{16}_X \to & \eta^x \left(\eta^{-3\gamma} L \oplus \eta^{3\gamma+\delta} e^c \oplus \eta^{3\gamma-\delta} N \oplus \eta^{-\gamma-\delta} u^c \oplus \right. \\ & \left. \oplus\ \eta^{-\gamma+\delta} d^c \oplus \eta^{\gamma} Q\right). \end{aligned} \tag{3.36}$$

Assuming $\overline{\mathbf{16}}_X$ transforms without Wilson line phases, $\overline{\mathbf{16}}_X \to \eta^{\overline{x}}\, \overline{\mathbf{16}}_X$, the condition for the mass term is

$$\overline{d^c}_X d^c_X : x - \gamma + \delta + \overline{x} = 0 \mod N, \tag{3.37}$$

whilst forbidding all the other self couplings that would arise from $\mathbf{16}_X \overline{\mathbf{16}}_X$.

The light D^w and $\overline{D}^w$ from the original $\mathbf{10}^w$ then "complete" the $\mathbf{16}_X + \overline{\mathbf{16}}_X$ pair, since they have the same SM quantum numbers as the missing $d^c_X, \overline{d^c}_X$. The light states in the $\mathbf{16}_X$ and $\overline{\mathbf{16}}_{\mathbf{X}}$ also obtain masses via the Kähler potential of order a TeV via the Giudice-Masiero mechanism. Gauge unification is clearly restored, albeit with a larger gauge coupling at the GUT scale due to the extra low energy matter content (relative to the MSSM).

Note that one can consider a model beyond simplicity by adding more vector-like multiplets which is consistent with anomaly cancellation constraints and gauge unification. However, such a model results in too large 1-loop gauge running coefficients so that the gauge couplings approach infinity before they unify. To avoid non-perturbativity issue, we are constrained to the model with $\mathbf{16}_X$ and $\overline{\mathbf{16}}_X$.

Effective μ-terms induced by moduli vevs of the form $\mu \mathbf{16}^m \overline{\mathbf{16}}_X$ are then gen-

erated and one might be concerned about too much mixing with quarks and leptons. However, one finds that all the light components of the extra matter decouple from ordinary matter, with mixings supressed by terms of order (3.32). For example, consider the up-type quark sector. The superpotential contribution to the mass matrix is, schematically, $U_L \cdot M_u \cdot U_R$, with $U_L = \begin{pmatrix} u^i & u_X & \overline{u^c}_X \end{pmatrix}^T$, $U_R = \begin{pmatrix} (u^c)^i & \overline{u}_X & u^c_X \end{pmatrix}^T$, and

$$M_u = \begin{pmatrix} y_u^{ij}\langle H_u\rangle & \mu^i_{XQ} & 0 \\ 0 & \mu_{XXQ} & 0 \\ \mu^j_{Xu} & 0 & \mu_{Xu} \end{pmatrix} \tag{3.38}$$

Here $\mu^i_{XQ}, \mu^j_{Xu}, \mu_{XXQ}$, μ_{Xu} are moduli induced μ-type parameters of $\mathcal{O}$(TeV) while the vanishing entries are non-zero only to first order in moduli-induced trilinear interactions that are vanishingly small, $\mathcal{O}(10^{-14})$. We have found numerically that flavour changing neutral currents (FCNCs) are highly suppressed by this structure. This can be understood analytically in the approximation that the electroweak masses can be ignored, since $y_u\langle H_u\rangle/\mu \sim \mathcal{O}(0.1)$. In this approximation, the third lightest u-quark will be given by the two component Weyl quarks

$$t = u_3' \simeq \frac{1}{\sqrt{(\mu^3_X)^2 + (\mu_{XXQ})^2}}((\mu_{XXQ})u_3 - (\mu^3_X)u_X), \tag{3.39}$$

$$t^c = (u^c_3)' \simeq \frac{1}{\sqrt{(\mu^3_{Xu})^2 + (\mu_{Xu})^2}}((\mu_{Xu}(u^c)_3 - (\mu^3_{Xu})u^c_X), \tag{3.40}$$

and as a result the light *up*-quark, which we denote t, does not result in a mixing including $\overline{u^c}_X$. This is important, since $\overline{u^c}_X$ in U_L couples to Z differently, only through the electromagnetic contribution to the neutral current and not via the J^μ_3 contribution. Consequently, FCNCs will be naturally suppressed and the CKM

matrix should have only small deviations from unitarity. Furthermore we note that the resulting matter states couple to the Higgses and Z as in the MSSM.

3.2.2 See-saw Mechanism

Introducing the $\mathbf{16}_X$ and $\overline{\mathbf{16}}_X$ will play a crucial role in breaking the extra $U(1)$ subgroup of $SO(10)$ and generating right-handed neutrino masses. We assume that a mechanism similar to the one proposed by Kolda-Martin [81] is in effect, such that the right-handed neutrino components acquire a non-trivial high-scale vev along the D-flat direction, $\langle N_X \rangle = \langle \overline{N}_X \rangle = v_X$, which in turn breaks the rank. However the scale v_X is constrained, as discussed below.

Presence of the $\mathbf{16}_X$ and $\overline{\mathbf{16}}_X$ with vevs in their right-handed neutrino components gives us the possibility of having a see-saw mechanism for light physical neutrino masses. Such a mechanism is welcome since representations larger than the $\mathbf{45}$ are absent in M theory [82]. In the present framework, a Majorana mass term for the right handed neutrino in $\mathbf{16}^m$ is generated by letting the discrete symmetry to allow the Planck suppressed operator $\frac{1}{m_{pl}}\overline{\mathbf{16}}_X\overline{\mathbf{16}}_X\mathbf{16}^m\mathbf{16}^m$. This requires charges to satisfy $2\overline{x} + 2\kappa = 0 \mod N$, and leads to the Majorana mass $M \sim \frac{{v_X}^2}{m_{pl}}$.

Due to the nature of $SO(10)$, the neutrinos will have the same Yukawa coupling as the up-type quarks y_u^{ij}, as in Eq. (3.29), leading to their Dirac masses being the same as the up-quark masses. For the case of the top quark mass we would need $M \sim 10^{14}$ GeV in order to give a realistic neutrino mass. Such a high value can only be achieved by the above see-saw mechanism if $v_X \gtrsim 10^{16}$ GeV.

The magnitude of v_X is also constrained by R-parity violating (RPV) dynamically generated operators, due to moduli and $N_X, \overline{N}_X$ vevs, arising from the

Kähler interactions

$$K_{RPV} \supset \frac{s}{m_{pl}^3}\mathbf{16}_X\mathbf{16}^m\mathbf{16}^m\mathbf{16}^m + \frac{s}{m_{pl}^2}\mathbf{10}^w\mathbf{16}_X\mathbf{16}^m. \tag{3.41}$$

Because moduli are also charged under the discrete symmetry, these operators are expected to be allowed due to generic charges of $\mathcal{O}(100)$ moduli. Since s and N_X acquire vevs, these operators generate the effective superpotential terms (otherwise forbidden by the discrete symmetry),

$$\begin{aligned} W_{RPV}^{eff} \supset\ & \lambda\frac{v_X}{m_{pl}}LLe^c + \lambda\frac{v_X}{m_{pl}}LQd^c + \lambda\frac{v_X}{m_{pl}}u^cd^cd^c + \\ & + \lambda v_X L H_u, \end{aligned} \tag{3.42}$$

with $\lambda \sim \mathcal{O}(10^{-14})$. One can absorb the last term into $\mu H_d H_u$ by a small rotation $\mathcal{O}(v_X/m_{pl})$ in (H_d, L) space,

$$W_{RPV}^{eff} \supset y_e\frac{v_X}{m_{pl}}LLe^c + y_d\frac{v_X}{m_{pl}}LQd^c + \lambda\frac{v_X}{m_{pl}}u^cd^cd^c, \tag{3.43}$$

where the first two terms originate from the Yukawa couplings $y_e H_d L e^c$, etc., and we have dropped the $\mathcal{O}(\lambda)$ contributions to these terms since now the Yukawa rotated contributions are much larger.

We emphasise that there exist explicit solutions to the constraints on all of the charges and couplings that we have discussed. These are Table 3.3, Eq. (3.37), the Majorana mass term, suppressing the RPV operators and cross-terms between the visible matter, 16_X and $16_{\overline{X}}$ necessary for Eq. (3.38). An example is given by

$$(N, \omega, \alpha, \beta, \kappa, x, \gamma, \delta, \overline{x}) = (16, 4, 0, 1, 6, 2, 1, 13, 2). \tag{3.44}$$

which is also anomaly free, as can be checked by explicit calculations [83].

The last term in Eq. (3.42) is the bilinear RPV operator which mixes the up-type Higgsino and neutrinos [84, 85]. The contribution to neutrino masses is tighly constrained leading to $\lambda v_X \lesssim \mathcal{O}(1\text{ GeV})$, which translates to the upper bound $v_X \lesssim 10^{14}$ GeV in contradiction with the see-saw requirement $v_X \sim 10^{16}$ GeV assumed in the above estimates. However, there is a natural way within this framework to further suppress the bilinear RPV terms. This happens when the charges of the moduli fields under the discrete symmetry are such that the leading order terms in K, which are linear in the moduli i.e. $\frac{s}{m_{pl}^2} v_X L H_u$, are *forbidden* by the symmetry, with the leading term arising at higher order in the moduli. If the leading term arises at cubic order or higher, (e.g. $K \sim \frac{s^3}{m_{pl}^4} v_X L H_u$ then the suppression will be sufficient. Furthermore, some moduli may have smaller vevs than others in a detailed model, leading to additional suppression.

The RPV terms in Eq. (3.43) induce the lightest supersymetric particle (LSP) decay. We can estimate its lifetime as [45]:

$$\tau_{LSP} \simeq \frac{3.9 \times 10^{-9}\,\text{sec}}{(v_X/m_{pl})^2} \left(\frac{m_0}{10\text{ TeV}}\right)^4 \left(\frac{100\text{ GeV}}{m_{LSP}}\right)^5 . \tag{3.45}$$

Since, as discussed above, $v_X/m_{pl} \sim 10^{-2}$, one finds $\tau_{LSP} \sim 10^{-4}\,\text{sec}$. This value is compatible with current bounds $\tau_{LSP} \lesssim 1$ sec [86], from Big Bang Nucleosynthesis. The result implies that the LSP is not a good dark matter candidate in M-theory framework. However, without the stable LSP, there are other possibility explaining dark matter in SO(10) models. As mentioned in the last chapter, axions from the string theory framework as a dark matter are the most common prediction [49, 50].

Note that in this framework, gravitino is not a candidate for dark matter since

it is not a stable particle with $\mathcal{O}(10)$ TeV mass. In fact the abundance of gravitino might be a problem to the BBN prediction as discussed before since its lifetime is of order $\frac{M_{pl}^2}{m_{3/2}^3} \sim 1$ sec. However, the decay of the lightest modulus generically produces a large amount of entropy such that the initial abundance of gravitino is diluted away. The gravitino thermal production from the lightest modulus is also found to be kinetically forbidden since we typically find that the lighest modulus is lighter than $2m_{3/2}$.

Since any global symmetries is explicitly broken from planck suppressed operators [70], there is no associated goldstone bosons such as R-axion from R-symmetry as a dark matter candidate.

Another possible solution would be an assumption that there exists a particle in a hidden sector that is lighter than the LSP and there is a portal between 2 sectors. In string/M theory framework, the portal connection is typically in the form of the kinetic mixing terms as argued in [87].

3.3 Conclusion

We have discussed the origin of an $SO(10)$ SUSY GUT from M theory on a G_2 manifold. We were naturally led to a novel solution of the doublet-triplet splitting problem involving an extra $\mathbf{16}_X + \overline{\mathbf{16}}_X$ vector-like pair where discrete symmetries of the extra dimensions were used to prevent proton decay by suppressing the Yukawa couplings of colour triplets. Such models maintain gauge coupling unification but with a larger GUT coupling than predicted by the MSSM. We argue that these extra multiplets, also required to break the additional $U(1)$ gauge symmetry, inevitably lead to significant R-parity violating effects when combining with the see-saw mechanism. Even though the moduli potential generically breaks the

discrete symmetry, we have seen that one naturally satisfies the constraints from the proton lifetime and decays affecting BBN. We also have found a consistent scenario for neutrino masses arising from the high scale see-saw mechanism, with sufficiently suppressed RPV contributions. We emphasise the main prediction of this approach, namely light states with the quantum numbers of a $\mathbf{16}_X + \overline{\mathbf{16}}_X$ vector-like pair which might be accessible in future LHC searches.

Chapter 4

Bottom-up Approach and Future Colliders

4.1 Introduction

In the MSSM, the chargino-neutralino sector is particularly important for several phenomenological reasons. Firstly, this sector contains Higgsinos, whose mass parameter, μ, plays a crucial role in electroweak symmetry breaking. If the MSSM provides a solution to the gauge hierarchy problem, at least some of the charginos and neutralinos must be present not too far from the electroweak scale. Secondly, many SUSY breaking scenarios suggest that one of the neutralinos becomes the lightest SUSY particle (LSP). Typically, the lightest neutralino is stable due to a discrete symmetry (e.g. R-parity) and might be a promising candidate for dark matter. Such a stable neutralino also plays a crucial role in collider phenomenology since the decay of supersymmetric particles will always produce the LSP, leading to a distinctive missing energy signature.

The ATLAS and CMS experiments at the CERN Large Hadron Collider (LHC)

have put considerable effort into looking for charginos and neutralinos in the LHC data. In hadron colliders the expected limit and discovery reach for the charginos and neutralinos are considerably weaker compared to those for squarks and gluinos. For the $\tilde{\chi}_1^\pm \tilde{\chi}_2^0 \to W^\pm \tilde{\chi}_1^0 Z \tilde{\chi}_1^0$ simplified model with $m_{\tilde{\chi}_1^\pm} = m_{\tilde{\chi}_2^0}$ and $m_{\tilde{\chi}_1^0} = 0$ GeV, the current limit is $m_{\tilde{\chi}_1^\pm} \gtrsim 400$ GeV [88,89]. The projection for the 14 TeV LHC has been estimated for the same simplified model by ATLAS [90]. The 5-σ discovery reach (95% CL limit) for the chargino mass is about 550 (880) GeV for 300 fb^{-1} and 800 (1100) GeV for 3000 fb^{-1}. For massive neutralinos ($m_{\tilde{\chi}_1^0} > 0$ GeV) or models with BR($\tilde{\chi}_2^0 \to h\tilde{\chi}_1^0$) > 0, the limit and discovery reach become even weaker. These limits are well below those required by typical dark matter models.

Recently, there has been discussion on the next generation of circular colliders, including high energy proton-proton machines. Several physics cases at proton-proton colliders with $\sqrt{s} \simeq 100$ TeV have already been studied [91–102]. In particular, the limit and discovery reach for coloured SUSY particles have been studied in the context of simplified models assuming a 100 TeV proton-proton collider with 3000 fb^{-1} of integrated luminosity [91]. The mono-jet search [96] as well as the mono-photon, soft lepton and disappearing track searches [100, 101] have been studied in the similar setup for production of the pure W-inos (Higgsinos), assuming they are the main component of the LSP. The 100 TeV colliders will provide a great opportunity to discover heavier charginos and neutralinos beyond the LHC reach.

In this chapter we investigate chargino-neutralino search at a 100 TeV collider assuming 3000 (1000) fb^{-1} luminosity exploiting the WZ channel. In stead of employing a simplified model approach, we work on a model which may arise as a limit of concrete models. In particular we assume $M_2 > \mu > 0$ and

$M_2 - \mu \gg m_Z$, where M_2 is the W-ino mass and μ is the Higgsino mass. In this scenario Higgsinos form the main component of the lighter charginos and neutralinos ($\tilde{\chi}_1^{\pm}, \tilde{\chi}_1^0, \tilde{\chi}_2^0 \sim \widetilde{H}^{\pm}, \widetilde{H}_1^0, \widetilde{H}_2^0$) and W-inos compose the heavier charginos and neutralinos ($\tilde{\chi}_1^{\pm}, \tilde{\chi}_3^0 \sim \widetilde{W}^{\pm}, \widetilde{W}^0$). This assumption is partly motivated by naturalness, by anomaly mediation SUSY breaking scenarios, by string/M theory models and by split supersymmetry [31, 32, 70, 103–108]

The assumption can also be realised in string/M theory framework. However in order to satisfy $M_2 > \mu > 0.1 m_{3/2}$, gaugino mass cannot be suppressed with respect to the gravitino mass. From the supergravity computation [75], the gaugino formula

$$m_{1/2} = \frac{e^{K/2} F^i \partial_i f_{vis}}{2i \mathrm{Im} f_{vis}} \tag{4.1}$$

implies that F-term of the geometric moduli appearing in the gauge kinetic function are not suppressed. This case could happen when the moduli are stabilised by string-loop effects or perturbative effects in Kahler potential [109].

The rest of the chapter is organised as follows. In section 4.2, we describe the model setup and study the production cross sections and branching ratios of charginos and neutralinos. After clarifying our simulation setup in section 4.3, various kinematic distributions for signal and background are studied in section 4.4, which will be used to design optimal event selection cuts for the chargino-neutralino search. In section 4.5, we present the result of our analysis and derive the limit and discovery reach in the $M_2 - \mu$ parameter plane. The conclusions are given in section 4.6.

4.2 The cross sections and branching ratios

4.2.1 The model setup

We focus on the models with $M_2 > \mu > 0$ and $M_2 - \mu \gg m_Z$, where the μ is the mass of the Higgsinos and M_2 is the mass of the W-inos since the W-ino production cross section is larger than the Higgsino cross section. We assume that all the other SUSY particles, including the B-ino, are decoupled and all SUSY breaking parameters are real for simplicity. In this situation the mixing between W-ino and Higgsino is negligible; the two Higgsino doublets are the lightest charginos and the two lightest neutralinos (which are almost degenerate) and the W-inos (SU(2) triplet) are the second lightest charginos and the third lightest neutralino (almost mass degenerate):

$$\begin{aligned} \tilde{\chi}_1^{\pm}, \tilde{\chi}_1^0, \tilde{\chi}_2^0 &\sim \widetilde{H}^{\pm}, \widetilde{H}_1^0, \widetilde{H}_2^0 \quad \text{with} \quad m_{\tilde{\chi}_1^{\pm}} \simeq m_{\tilde{\chi}_1^0} \simeq m_{\tilde{\chi}_2^0} \simeq |\mu|, \\ \tilde{\chi}_2^{\pm}, \tilde{\chi}_3^0 &\sim \widetilde{W}^{\pm}, \widetilde{W}^0 \quad \text{with} \quad m_{\tilde{\chi}_2^{\pm}} \simeq m_{\tilde{\chi}_3^0} \simeq |M_2|, \end{aligned} \tag{4.2}$$

where $\widetilde{H}_{1/2}^0 = \frac{1}{\sqrt{2}}(\widetilde{H}_u^0 \mp \widetilde{H}_d^0)$ is the neutral Higgsino mass eigenstate. With this setup, the remaining free parameters are M_2, μ and $\tan\beta$. We use $\tan\beta = 10$ throughout our numerical study. We give examples of the mass spectrum and splittings in table 4.1.

However, the impact of $\tan\beta$ on the production cross section and branching ratio of the charginos and neutralinos that are W-ino or Higgsino like is almost negligible unless $\tan\beta$ is extremely small. The $\tan\beta$ dependence of the cross section is shown in figure 4.2. We therefore believe our results including the chargino-neutrino mass reach are still useful for other values of $\tan\beta$.

M_2 [GeV]	μ [GeV]	$\tan\beta$	$\tilde{\chi}_1^0$ [GeV]	$\tilde{\chi}_2^0$ [GeV]	$\tilde{\chi}_1^\pm$ [GeV]	$\tilde{\chi}_3^0$ [GeV]	$\tilde{\chi}_2^\pm$ [GeV]
1500	1200	5	1185.8	1200.8	1192.0	1514.8	1508.0
1500	1200	10	1187.6	1202.0	1195.8	1513.18	1504.2
1500	1200	50	1189.2	1201.2	1199.1	1511.8	1599.9
2500	1200	5	1196.5	1200.6	1198.1	2503.9	2501.9
2500	1200	10	1196.9	1200.7	1199.0	2503.6	2501.0
2500	1200	50	1197.3	1200.9	1200.0	2503.4	2500.2
3500	1200	5	1198.0	1200.5	1199.0	3502.3	3501.1
3500	1200	10	1198.2	1200.6	1199.5	3502.2	3500.6
3500	1200	50	1198.4	1200.7	1199.9	3502.1	3500.1

Table 4.1: The mass spectrum for various benchmarks. Notice that $\tan\beta$ dependence on the mass spectrum is mostly neglible and the degeneracies appearing in 4.2 is valid up to soft activities.

4.2.2 The cross sections

We show the leading order (LO) cross sections for the W-ino and Higgsino pair productions at a 100 TeV proton-proton collider in figure 4.1. The cross sections are calculated using `MadGraph 5` [110]. Since squarks are decoupled, the W-inos and Higgsinos are produced via the s-channel diagrams exchanging off-shell $W^\pm$ and Z bosons. For the pure W-inos and Higgsinos, there is no associated W-ino-Higgsino production process. Pair production of the same neutralino states, $\widetilde{W}^0\widetilde{W}^0$, $\widetilde{H}_1^0\widetilde{H}_1^0$, $\widetilde{H}_2^0\widetilde{H}_2^0$, are also absent.

One can see that the $\widetilde{W}^\pm\widetilde{W}^0$ production mode has the largest cross section. The LO cross section varies from 10^3 fb to 10^{-2} fb for the W-ino mass from 500 GeV to 8 TeV.

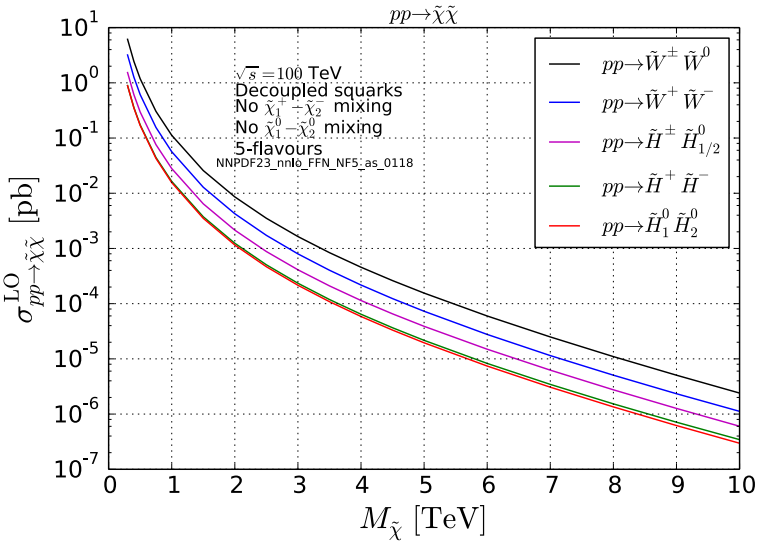

Figure 4.1: The leading order cross sections for the W-ino and Higgsino pair productions at a 100 TeV proton-proton collider with decoupled squarks and sleptons.

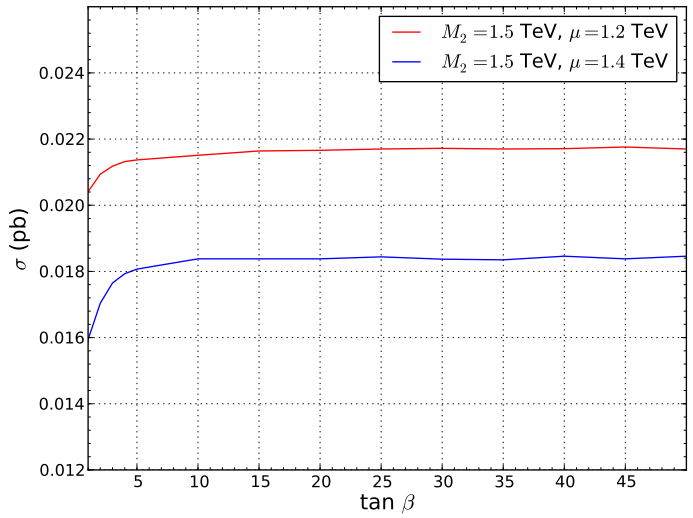

Figure 4.2: The cross sections for the $\tilde{\chi}_2^{\pm}\tilde{\chi}_3^0 \sim \widetilde{W}^{\pm}\widetilde{W}^0$ production as a function of $\tan\beta$.

4.2.3 The branching ratios

The W-ino-Higgsino interaction is derived from the kinetic terms of Higgsinos.

$$\begin{aligned}\mathcal{L} &\supset \left[H_u^\dagger e^V H_u + H_d^\dagger e^V H_d\right]_{\theta^4} \\ &\supset \sqrt{2}g(H_u^* \widetilde{W}^a T^a \widetilde{H}_u - H_d^* \widetilde{W}^a T^a \widetilde{H}_d) + \text{h.c.} \end{aligned} \tag{4.3}$$

The Higgs and Higgsino fields can be written in terms of the Goldstone bosons and the mass eigenstates as:

$$\begin{pmatrix} H_u^+ \\ H_u^0 \end{pmatrix} = \begin{pmatrix} \sin\beta \cdot \phi^+ + \cdots \\ \frac{1}{\sqrt{2}}(\cos\alpha \cdot h + i \sin\beta \cdot \phi^0) + \cdots \end{pmatrix}, \quad \begin{pmatrix} \widetilde{H}_u^+ \\ \widetilde{H}_u^0 \end{pmatrix} \simeq \begin{pmatrix} \widetilde{H}^+ \\ \frac{1}{\sqrt{2}}(\widetilde{H}_1^0 + i\widetilde{H}_2^0) \end{pmatrix},$$

$$\begin{pmatrix} H_d^0 \\ H_d^- \end{pmatrix} = \begin{pmatrix} \frac{-1}{\sqrt{2}}(\sin\alpha \cdot h + i \cos\beta \cdot \phi^0) + \cdots \\ -\cos\beta \cdot \phi^- + \cdots \end{pmatrix}, \quad \begin{pmatrix} \widetilde{H}_d^0 \\ \widetilde{H}_d^- \end{pmatrix} \simeq \begin{pmatrix} \frac{1}{\sqrt{2}}(\widetilde{H}_1^0 - i\widetilde{H}_2^0) \\ \widetilde{H}^- \end{pmatrix}, \tag{4.4}$$

where h is the SM like Higgs boson, and ϕ^0 and $\phi^\pm$ are the Goldstone bosons to be eaten by the SM gauge bosons, Z and $W^\pm$, respectively. The angles α and β represent the mixing for the neutral and charged Higgs mass matrices.

In the large $\tan\beta$ limit, we have $\cos\alpha/\sin\alpha \simeq (-\sin\beta)/\cos\beta$, and one can see that the $h\widetilde{W}\widetilde{H}$, $\phi^0\widetilde{W}\widetilde{H}$ and $\phi^\pm\widetilde{W}\widetilde{H}$ have the same coupling. In this limit one

can find the following results using the Goldstone equivalence theorem [111].

$$\begin{aligned}
\mathrm{BR}(\widetilde{W}^{\pm}) &\simeq \begin{cases} 0.5 & \to W^{\pm}\widetilde{H}_1^0 \text{ or } W^{\pm}\widetilde{H}_2^0 \\ 0.25 & \to h\widetilde{H}^{\pm} \\ 0.25 & \to Z\widetilde{H}^{\pm} \end{cases} \\
\mathrm{BR}(\widetilde{W}^{0}) &\simeq \begin{cases} 0.5 & \to W^{\pm}\widetilde{H}^{\mp} \\ 0.25 & \to h\widetilde{H}_1^0 \text{ or } h\widetilde{H}_2^0 \\ 0.25 & \to Z\widetilde{H}_1^0 \text{ or } Z\widetilde{H}_2^0 \end{cases}
\end{aligned} \tag{4.5}$$

The different CP properties between h and ϕ^0, and $\widetilde{H}_1^0$ and $\widetilde{H}_2^0$ result in the different rates for $\widetilde{W}^0 \to h\widetilde{H}_1^0$ and $\widetilde{W}^0 \to Z\widetilde{H}_1^0, h\widetilde{H}_2^0$. These rates are given by

$$\begin{aligned}
\mathrm{BR}(\widetilde{W}^{\pm} \to W^{\pm}\widetilde{H}_1^0) &\simeq \mathrm{BR}(\widetilde{W}^{\pm} \to W^{\pm}\widetilde{H}_2^0), \\
\mathrm{BR}(\widetilde{W}^{0} \to h\widetilde{H}_{1/2}^0) &\simeq \mathrm{BR}(\widetilde{W}^{0} \to Z\widetilde{H}_{2/1}^0), \\
\frac{\mathrm{BR}(\widetilde{W}^{0} \to Z\widetilde{H}_1^0)}{\mathrm{BR}(\widetilde{W}^{0} \to h\widetilde{H}_1^0)} &\simeq \frac{1-2|\mu/M_2|}{1+2|\mu/M_2|} \,.
\end{aligned} \tag{4.6}$$

Figure 4.3 shows the branching ratios of $\widetilde{W}^{\pm}$ and $\widetilde{W}^0$, which have been calculated using `SUSY-HIT` [112]. One can see that the branching ratios approach eq. (4.5) in the large M_2 limit. For the region where $|M_2 - \mu|$ is close to the masses of SM bosons, the decay mode into $W^{\pm}$ enhances since it has the largest phase space factor.

Since the charged and neutral W-inos are almost mass degenerate, it may not be possible to resolve $\widetilde{W}^{\pm} \to XY$ and $\widetilde{W}^0 \to X'Y'$ in hadron colliders if XY is equal to $X'Y'$ up to soft activities. Similarly, four degenerate Higgsinos would not be resolvable, since $\widetilde{H}^{\pm}$ and $\widetilde{H}_2^0$ usually decay promptly into $\widetilde{H}_1^0$ and their decay products are too soft to be detected. We therefore categorise the

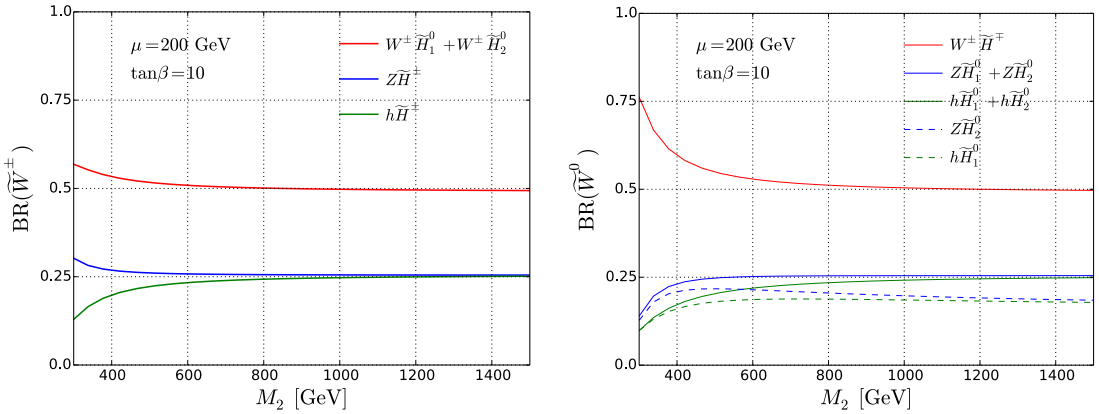

Figure 4.3: The branching ratios of $\widetilde{W}^{\pm}$ **(a)** and $\widetilde{W}^0$ **(b)** as functions of M_2. The μ parameter is fixed at 200 GeV. The SUSY particles other than W-inos and Higgsinos are decoupled.

processes into distinguishable groups in terms of the SM bosons appearing in the final states. For example, $\chi'\chi' \to WZ\chi\chi$ process (WZ mode) includes $\widetilde{W}^+\widetilde{W}^- \to (W^{\pm}\widetilde{H}^0_{1/2})(Z\widetilde{H}^{\mp})$, $\widetilde{W}^{\pm}\widetilde{W}^0 \to (W^{\pm}\widetilde{H}^0_{1/2})(Z\widetilde{H}^0_{1/2})$, $(Z\widetilde{H}^{\pm})(W^{\pm}\widetilde{H}^{\mp})$ and $\widetilde{W}^0\widetilde{W}^0 \to (W^{\pm}\widetilde{H}^{\mp})(Z\widetilde{H}^0_{1/2})$. We show the cross sections of the all 6 distinguishable modes, WZ, Wh, WW, ZZ, Zh and hh modes, in the $M_2 - \mu$ plane in figure 4.4.

One can see that the modes containing at least one W have considerably larger cross sections compared to the others at the same mass point. In particular, the WZ mode is promising[1] because one can reduce the QCD and $t\bar{t}$ backgrounds significantly by requiring three high p_T leptons (see figure 4.5). Taking advantage of this we henceforth study the expected discovery reach and exclusion limit for chargino-neutralino production in the WZ mode.

In figure 4.6, we show the cross section of the WZ mode after taking account of the branching ratios of the gauge bosons into $3\ell + \nu$. The black curve represents the limit beyond which less than 5 signal events ($\chi'\chi' \to WZ\chi\chi \to 3\ell\nu\chi\chi$)

[1]The Wh mode is also interesting. See [113–117] for some recent studies.

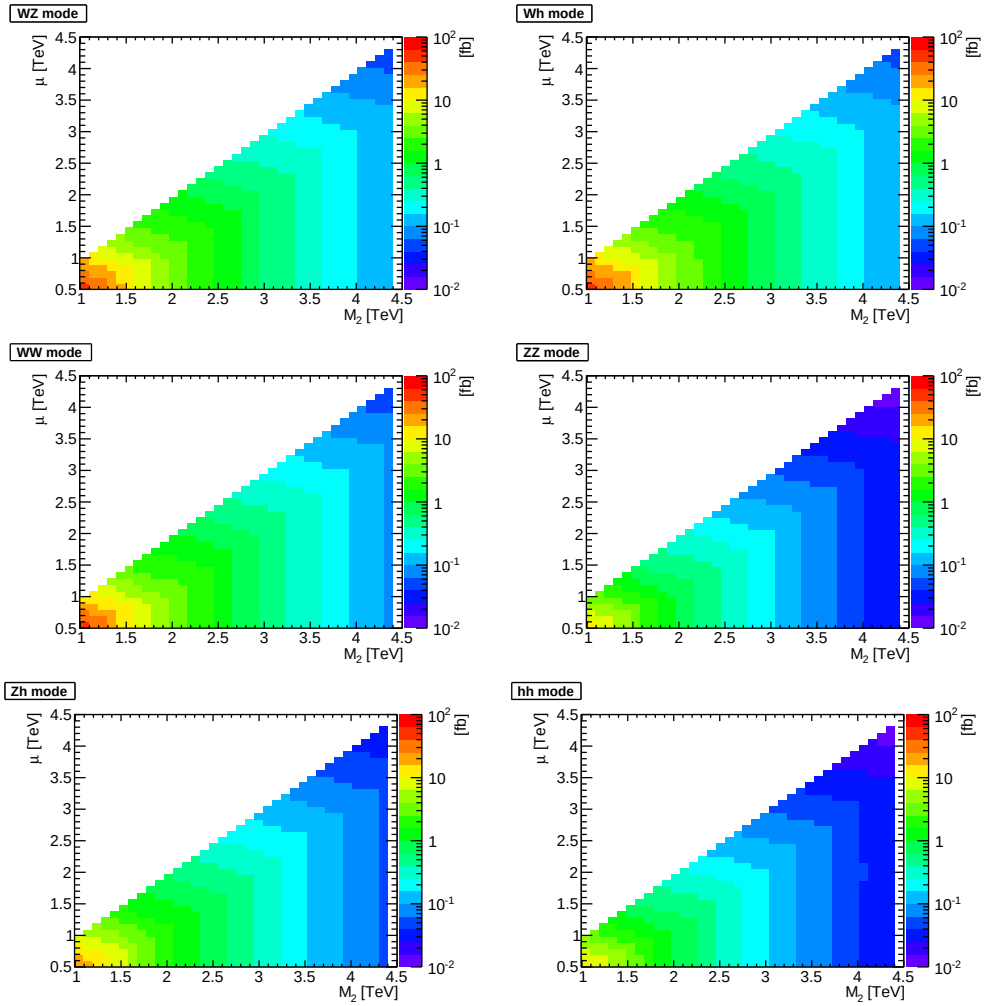

Figure 4.4: The cross sections of the 6 distinguishable modes, $\chi'\chi' \to XY\chi\chi$ with $XY = WZ, Wh, WW, ZZ, Zh$ and hh, as functions of M_2 and μ. SUSY particles other than W-inos and Higgsinos are decoupled.

are produced, assuming the integrated luminosity of 3000 fb^{-1}. This provides a rough estimate of the theoretically maximum possible exclusion limit assuming zero background with perfect signal efficiency.

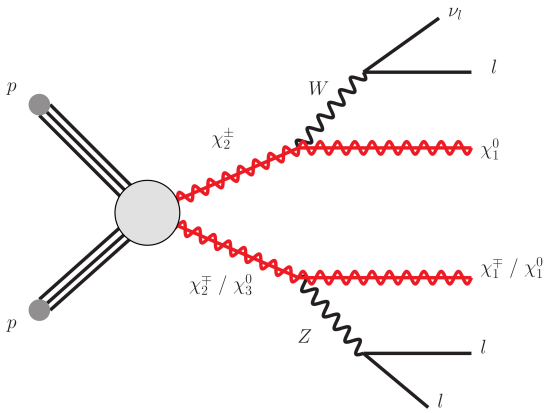

Figure 4.5: The dominant event topology for signal events.

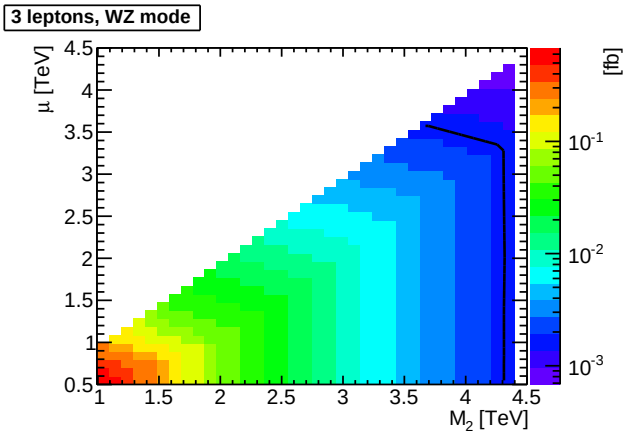

Figure 4.6: The cross section of $\chi'\chi' \to WZ\chi\chi \to 3\,\ell\nu\chi\chi$ as a function of M_2 and μ. The black curve represents the limit beyond which less than 5 signal events are produced, assuming the integrated luminosity of 3000 fb^{-1}.

4.3 The simulation setup

We use the Snowmass background samples [118] to estimate the Standard Model (SM) backgrounds. We include the relevant SM processes, which are summarised in table 4.2.

For signal events we first generate chargino and neutralino production events using `MadGraph 5` with the parameters obtained by `SUSY-HIT`. We consider two

Name	Snowmass	Relevant sub-processes	$\sigma^{\rm NLO}_{\rm total}$ [pb]
diboson	VV	W^+W^-, $W^\pm Z$, ZZ	3298.4
top-pair + gauge boson	ttV	$t\bar{t}W^\pm$, $t\bar{t}Z$, $t\bar{t}\,h$	219.9
top + gauge boson	tV	$tW^\pm$, $\bar{t}W^\pm$	3582.2
triple gauge boson	VVV	$W^+W^-W^\pm$, W^+W^-Z, $W^\pm ZZ$, ZZZ	36.4

Table 4.2: The Standard Model background included in the analysis. For each background category, we only list sub-processes relevant in the 3 lepton analysis. Reported cross sections include all sub-processes in corresponding background categories.

production processes $pp \to \chi_2^+\chi_2^-$ and $pp \to \chi_2^\pm\chi_3^0$, where $\chi_2^\pm \sim \widetilde{W}^\pm$ and $\chi_3^0 \sim \widetilde{W}^0$. The generated samples are then passed to `BRIDGE` [119] to have the charginos and neutralinos decay. We then only accept the events with W and Z in the final states, and pass those events once again to `BRIDGE` to let W and Z decay leptonicaly. Finally we simulate the effects of parton shower, hadronization and detector resolutions using `Pythia 6` [120] and `Delphes 3` [121]. The detector simulation is tuned according to the Snowmass detector framework [118].

4.4 The kinematic distributions

In this section we show some kinematic distributions for the background and signal events. We consider the WZ mode for signal and diboson (VV) and top-pair plus gauge boson (ttV) processes for backgrounds. The signal distributions are generated at a benchmark point: $M_2 = 1.4$ TeV, $\mu = 200$ GeV. Throughout this section we use a notation denoting the i-th hardest lepton (electron or muon) by ℓ_i (namely, $p_T(\ell_i) > p_T(\ell_j)$ for $i < j$).

Figure 4.7(a) shows the normalised distributions of the leading lepton pseudo-rapidity, η_{ℓ_1}, for signal (black) and background (red for VV and green for ttV). The distributions are obtained at a parton level without selection cuts apart from

$p_T(\ell_1) > 10$ GeV to understand the bare distribution before taking the detector acceptance into account. One can see that the leptons in the background tend to be more forward compared to the signal leptons. The production threshold is much lower for the backgrounds and more asymmetric momentum configurations are allowed for the initial partons. If one of the initial partons has a much larger momentum than the other, the system is boosted in the direction of the beam pipe and the leptons tend to be produced in the forward region.[2] Another effect is as follows. Unlike the signal, production of the backgrounds have a contribution from t-channel diagrams. In 100 TeV colliders, the SM gauge bosons can effectively be regarded as "massless" particles and there is an enhancement in the region of the phase space where the gauge bosons are produced in the forward region.

Figure 4.7(b) shows the p_T distributions of the three hardest leptons. The distributions are obtained after taking the hadronization and detector effects into account and requiring at least 3 leptons (with $p_T > 10$ GeV, $|\eta| < 2.5$), of which two are same flavour and opposite sign (SFOS). As can be seen, the p_T-spectrum of background leptons has peaks below 100 GeV, whilst the signal peaks at around 300, 150 and $\lesssim 50$ GeV for the leading, second leading and third leading leptons for our benchmark point.

We also show the $E_T^{\rm miss}$ distributions in figure 4.7(c), where we use the same event sample as those in figure 4.7(b). The main source of the $E_T^{\rm miss}$ in the background are the neutrinos produced from W and Z decays and the distribution has a peak around 30−40 GeV. Above this peak, the background $E_T^{\rm miss}$ distribution falls quickly. On the other hand, a large $E_T^{\rm miss}$ can be produced from the signal from the decays of heavy charginos and neutralinos. The typical scale of $E_T^{\rm miss}$

[2]For the W^+Z background, the initial state is often u and $\bar{d}$. If the partonic collision energy is much smaller than the proton-proton collision energy, it is more likely to find a valence quark u carrying a larger fraction of the proton momentum compared to the sea quark $\bar{d}$.

is given by $\sim M_2/2$. As can be seen, the signal distribution has a peak around 500 GeV. This indicates that a hard cut on $E_T^{\rm miss}$ will greatly help to improve the signal to background ratio.

We show the transverse mass m_T distributions in figure 4.7(d), where the event samples are again the same as those used in figure 4.7(b). We define $m_T \equiv \sqrt{2|p_T(\ell')||E_T^{\rm miss}|(1-\cos\Delta\phi)}$, where ℓ' is the hardest lepton amongst those not chosen as the SFOS lepton pair and $\Delta\phi$ is the azimuthal difference between the ℓ' and the direction of $\overrightarrow{p}_T^{\rm miss}$. In the WZ background, this distribution has an endpoint at m_W and above the endpoint the distribution drops very sharply. In the signal events, the distributions are much broader, as can be seen in figure 4.7(d). A harsh cut on m_T would also be very helpful to reject a large fraction of background without sacrificing too many signal events.

4.5 The limit and discovery reach

4.5.1 The event selection

Our event selection consists of two parts: *preselection* and *signal region* (SR) *selection*. The *preselection* requirement is:

- exactly three isolated leptons with $p_T > 10$ GeV and $|\eta| < 2.5$,
- a same-flavour opposite-sign (SFOS) lepton pair with $|m_{\ell\ell}^{\rm SFOS} - m_Z| < 10$ GeV,
- no b-tagged jet.

With the first condition one can effectively reject the QCD, hadronic $t\bar{t}$ and single gauge boson backgrounds. The definition of lepton isolation and some discussion

Signal Region	3 lepton p_T [GeV]	$E_T^{\rm miss}$ [GeV]	m_T [GeV]
Loose	$> 100, 50, 10$	> 150	> 150
Medium	$> 250, 150, 50$	> 350	> 300
Tight	$> 400, 200, 75$	> 800	> 1100

Table 4.3: The event selection cuts required in the signal regions. These cuts are applied on top of the preselection cuts.

around it is given in Appendix A.2. The second condition is introduced to remove the leptonic SM processes without Z bosons, such as $t\bar{t}W^{\pm}$ and $W^+W^-W^{\pm}$. The last condition is effective to reduce the SM backgrounds containing top quarks. In the simulation we use the b-tagging efficiency of about 70 %, which is set in the `Delphes` card used in the Snowmass backgrounds.

In order to obtain as large coverage as possible in the $M_2 - \mu$ parameter plane, we define three signal regions: *Loose*, *Medium*, *Tight*. These signal regions are defined in table 4.3. The selection cuts are inspired by the kinematical distributions shown in figure 4.7. The *Loose* region, which has the mildest cuts, is designed to constrain the degenerate mass region ($M_2 \gtrsim \mu$), whereas the *Tight* region, which has the hardest cuts, targets the hierarchical mass region ($M_2 \gg \mu$). The *Medium* region is also necessary to extend the coverage in the intermediate mass region.

The visible cross section (the cross section for the events satisfying the event selection requirements) for each signal region is shown in Appendix A.3. The information for the detailed breakdown of the background contribution and the visible cross section at each step of the selection is also shown. The number of total background events are expected to be 38400, 810 and 12.3 for the *Loose*, *Medium* and *Tight* signal regions, respectively, at 3000 fb^{-1} of integrated luminosity.

4.5.2 The result

In figure 4.8(a), we show the $2\,\sigma$ exclusion limits in the $\mu - M_2$ parameter plane obtained by the different signal regions. The shaded regions have $S/\sqrt{B} \geq 2$, where S and B are the number of expected signal and background events falling into the signal regions, respectively. For signal we use a constant k-factor of 1.3 across the parameter plane. One can see that the three signal regions are complementary and M_2 can be constrained up to ~ 1.8 TeV for $\mu \lesssim 800$ GeV.

Figure 4.8(b) shows the $5\,\sigma$ discovery reach ($S/\sqrt{B} \geq 5$) obtained from the different signal regions. As can be seen, the *Loose* and *Medium* signal regions provide the discovery reach up to about 850 and 1.1 TeV, respectively, for $\mu \lesssim 450$ GeV. On the other hand, the *Tight* signal region does not have sensitivity to $S/\sqrt{B} \geq 5$.

We show in figure 4.9(a) the global $2\,\sigma$ exclusion limits for integrated luminosities of 3000 fb^{-1} (red) and 1000 fb^{-1} (blue). The global exclusion limit is obtained by choosing the signal region that provides the largest $S/\sqrt{B}$ for each mass point. The shaded regions around the solid curves represent the uncertainty when varying the background yields by $\pm 30\,\%$. One can see that changing the background by $30\,\%$ results in a ~ 100 GeV shift in M_2 for the $\mu \ll M_2$ region. M_2 can be constrained up to 1.8 TeV with $\mu \lesssim 800$ GeV for 3000 fb^{-1}, which can be compared with the projected chargino neutralino mass limit of 1.1 TeV for the high luminosity LHC with 3000 fb^{-1} obtained by ATLAS [90]. For 1000 fb^{-1} the limit on M_2 is about 1.5 TeV with $\mu \lesssim 400$ GeV as can be seen in figure 4.9(a).

Figure 4.9(b) shows the global $5\,\sigma$ discovery reach for 3000 fb^{-1} (red) and 1000 fb^{-1} (blue) with the $30\,\%$ uncertainty bands for background. One can see that charginos and neutralinos can be discovered up to $M_2 \lesssim 1.1$ TeV with $\mu \lesssim 500$ GeV for 3000 fb^{-1} integrated luminosity, which can be compared with the pro-

jected ATLAS value of 0.8 TeV for the high luminosity LHC [90]. For 1000 fb^{-1}, charginos and neutralinos can be discovered up to 900 GeV with $\mu \lesssim 250$ GeV.

Note that in our simulation we include both the WZ and ZZ modes in the signal sample, though the contribution from ZZ mode is typically less than about 5 % after the selection cuts. We have also investigated the contribution from the other modes and found these to be of order ~ 10 % or less, predominantly from Zh. This can therefore be considered as a small uncertainty on the discovery limit.

4.6 Conclusion

We studied the prospect of chargino and neutralino searches at a 100 TeV pp collider assuming 3000 (1000) fb^{-1} of integrated luminosity. Our particular focus was the case where the Higgsinos form the lightest SUSY states (the lightest charginos and the two lightest neutralinos, which are almost mass degenerate) and W-inos form the second lightest states (the heavier charginos and the third lightest neutralino, which are almost mass degenerate). The other SUSY particles including B-ino are assumed to be decoupled, which is partly motivated by the current LHC results as well as popular scenarios of SUSY breaking and its mediation. We have shown that in this situation the LO production cross sections of 2 TeV W-inos are as large as 100 fb^{-1} and the branching ratio of W-inos follows a simple formula, which can be derived from the Goldstone equivalence theorem.

From a study of kinematic distributions of signal and background we found harsh cuts on lepton p_T ($> 50 - 400$ GeV), $E_T^{\rm miss}$ ($> 150 - 800$ GeV) and m_T ($> 150 - 1100$ GeV) are beneficial to improve the signal and background ratio and designed three complementary signal regions. Using these three signal regions,

we found the $5\,\sigma$ discovery reach ($2\,\sigma$ exclusion limit) for the chargino-neutralino mass is 1.1 (1.8) TeV for $\mu \lesssim 500$ (800) GeV, which can be compared with the projected LHC reach (limit) of 0.8 (1.1) TeV obtained by ATLAS [90]. For 1000 fb^{-1} the discovery reach (exclusion limit) for the chargino-neutralino mass is found to be 0.9 (1.5) TeV for $\mu \lesssim 250$ (400) GeV.

We would also like to comment on other hierarchies in the chargino-neutralino spectrum. In this study we have focused on a particular hierarchy ($|M_2| \gg |\mu|$) of the W-ino and Higgsino states. If the LSP is a W-ino and the Higgsinos are not decoupled, one can consider the Higgsino pair production process followed by the decay of Higgsinos into the W-inos. As can be seen from figure 4.1, the chargino-neutralino production has the largest cross section similarly to the W-ino production case, though the size of the cross section is about 5 times smaller compared to the W-ino production. Moreover the same argument based on the Goldstone equivalence theorem still holds for the Higgsino decay modes and leads to $Br(\tilde{H}^0_{1/2} \to Z\tilde{W}^0)/Br(\tilde{H}^0_{1/2} \to h\tilde{W}^0) \sim 1$. Therefore, the most promising channel in this scenario is again WZ + missing energy final state and they are effectively searched for by the 3-lepton analysis we have proposed in this work.[3] The same argument applies for the B-ino LSP case with non-decoupled Higgsinos.

Note added: There is a similar study in [122]. The authors considered a variable: $H_T(\text{jets})/M_{eff}$, where $H_T(\text{jets})$ is the scalar sum of all reconstructed jet p_T's and M_{eff} is the sum of all reconstructed object p_T's. This ratio is very useful to discriminate the chargino-neutralino signal from background. We have checked that adding this variable to our event selection improves our exclusion limit (discovery reach) by 200 (300) GeV if the detector simulation is taken into account and the effective lepton separation of $\Delta R = 0.3$ is used. The authors

[3]For a concrete study, see [122].

of [122] used a milder lepton isolation criteria and their study is without a detector simulation.

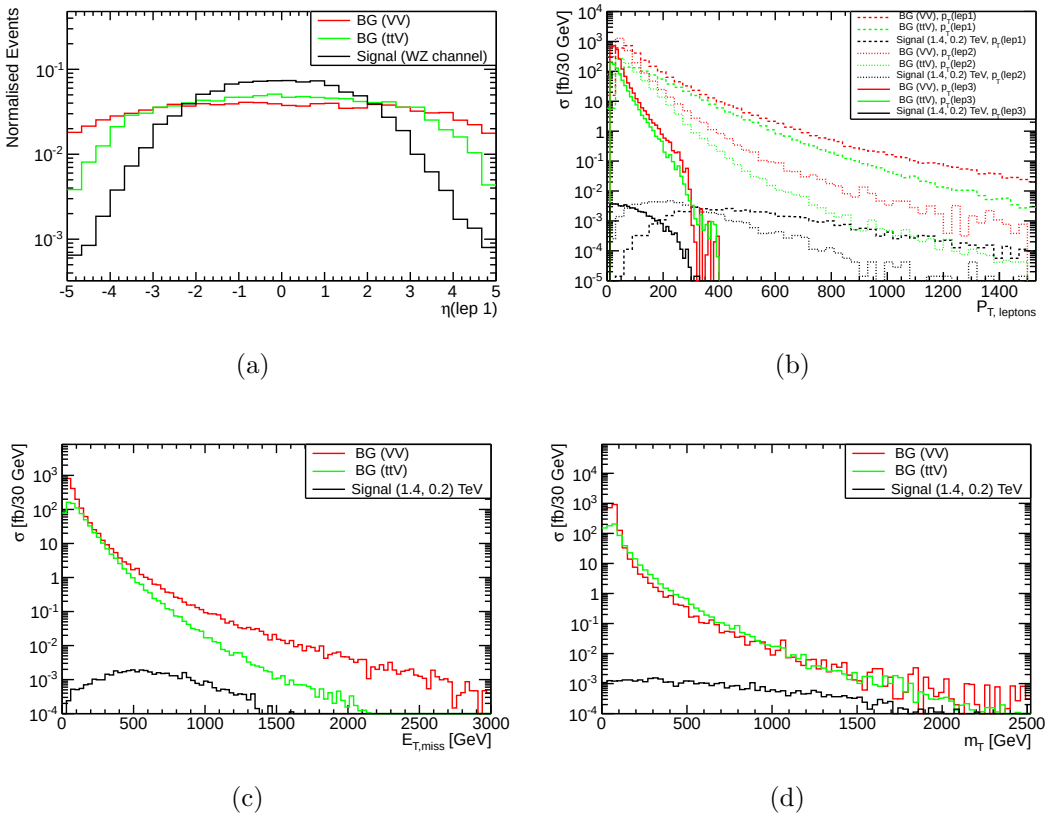

(a) (b)

(c) (d)

Figure 4.7: The distributions before the selection cuts of **(a)** the leading lepton pseudo-rapidity, η_{ℓ_1}, **(b)** p_T of the three hardest leptons, **(c)** the missing transverse energy, E_T^{miss}, **(d)** the transverse mass, m_T. The backgrounds are diboson (VV) and associated top-pair plus vector boson production (ttV). The signal events are generated at our benchmark point, $M_2 = 1.4$ TeV and $\mu = 200$ GeV, and only WZ mode is considered. The parton level events are used for **(a)**, whilst the detector level events after applying the 3 lepton + SFOS cuts are used for **(b)**, **(c)** and **(d)**.

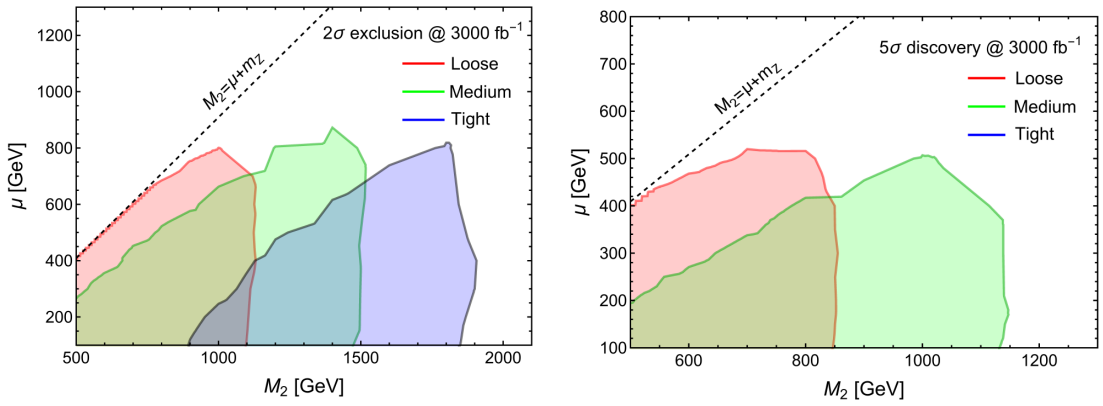

(a) (b)

Figure 4.8: The exclusion limits **(a)** and the discovery reaches **(b)** obtained from three signal regions. As discussed before, the value of $\tan\beta$ has no impact on the result unless $\tan\beta$ is extremely small. We used $\tan\beta = 10$ in this plot. The integrated luminosity of 3000 fb^{-1} is assumed.

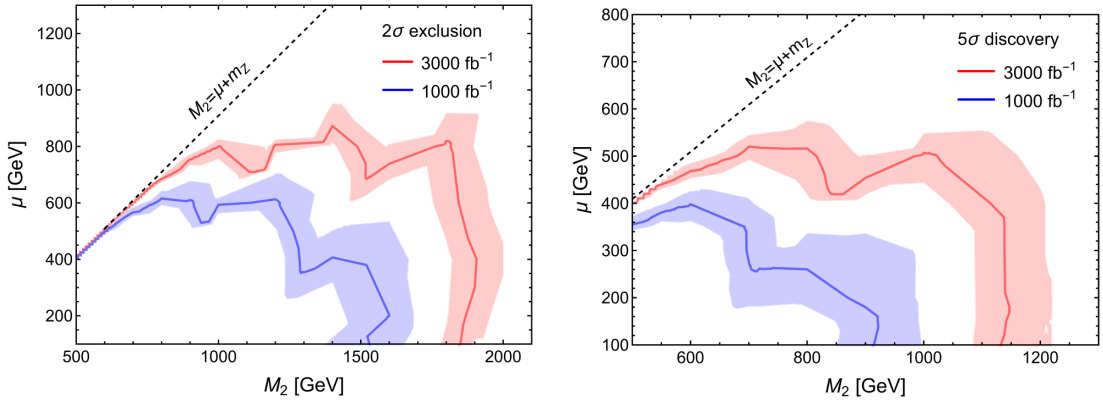

(a) (b)

Figure 4.9: The global exclusion limits **(a)** and the discovery reaches **(b)** for 3000 fb^{-1} (red) and 1000 fb^{-1} (blue). The shaded region represent the uncertainty when varying the background yield by 30 %.

Chapter 5

Conclusions

Motivated by recent developments in string compactification, string/M theory can make a connection with low energy physics giving interesting phenomenologies. In this thesis, we take a point of view that our universe is in fact a solution of string/M theory and explore various phenomenological consequences.

We argue that dark radiation is very useful in offering a powerful test on string/M theory framework. Due to the smallness of an observable such as ΔN_{eff}, a light degree of freedom coming from string compactification is severely constrained. We investigate the dark radiation constraint in the Axiverse scenario and provide several possible mechanisms in which the problem might be alleviated. First, a relatively large vev of a particular modulus can suppress the axion contribution to the dark radiation density. However, since large moduli vevs correspond to a weak standard model coupling, it might be difficult to make the vev large enough without making the standard model coupling too small. Another solution might be an alignment between the axion kinetic and mass mixing matrices so that the lightest modulus decays mainly to its axionic partner.

We also explore the model building aspect of string phenomenology. We study

the origin of an $SO(10)$ SUSY GUT from M theory on a G_2 manifold. A discrete symmetry non-commuting with $SO(10)$ constructing from Witten's proposal can be used to solve the doublet-triplet splitting problem where yukawa couplings of colour triplets are suppressed. Including an extra $\mathbf{16}_X + \overline{\mathbf{16}}_X$ vector-like pair restores the gauge coupling unification with a larger GUT coupling than predicted by the MSSM. We also study R-parity violating operators from the model and found that the constraints from the proton lifetime and decays affecting BBN are naturally satisfied. The RPV contribution to neutrino masses can be suppressed.

We also present results from a physics study of a future proton-proton collider. Motivated by string/M theory framework, we investigate searches for chargino-neutralino at a 100 TeV collider assuming 3000 fb^{-1} luminosity. We focus particularly on the scenario where Higgsinos mainly form the lightest charginos/neutralinos and Winos mainly form the second lightest charginos/neutralinos. We found that the WZ channel ($\chi'\chi' \to WZ\chi\chi$) is promising because the QCD background and $t\bar{t}$ are reduced sinificantly by requiring three high p_T leptons. We compare signal and background in various kinematical distributions and design signal regions for the trilepton channel and evaluate discovery/exclusion limits. Assuming 3000 fb^{-1} luminosity, Winos could be discovered up to 1.1 TeV if the spectrum is not compressed.

There are possible directions for future research. From theoretical point of view, it would be very interesting to exploit the mechanisms we learned from Axivere-induced dark radiation problem. The study could galvanize a new idea on a string compactification consistent with the Axiverse scenario. Within the reach of the LHC and future colliders, the new physics is most likely to be discovered. It is therefore crucial to pin down string/M theory frameworks from the the top-down and bottom-up approach with equal importance. Within the

model $SO(10)$ GUT from M theory compactified on a G_2 manifold we studied, extra states such as those of $\mathbf{16}_X + \overline{\mathbf{16}}_X$ might be accessible. The study of the extra $U(1)$ symmetry breaking is also very important for R-parity violation and neutrino physics. Moreover, the understanding of the $SO(10)$ case can be easily generalised to a larger gauge group such as E_6 or E_8. From a bottom-up perspective, the potential of the next generation colliders which has been widely discussed is very exciting. The detailed study of physics scenarios in future machines might eventually provide a powerful test on our understanding of particle physics from string/M framework.

Appendix A

Appendices

A.1 N_{eff} calculation

In this section, we compute the effective number of neutrinos in order to address the dark radiation problem. At the time of Big Bang Nucleosynthesis, the effective number of neutrinos is defined from

$$\rho_{rad} = \rho_{e^{\pm}} + \rho_{\gamma} + N_{eff}\rho_{\nu} \tag{A.1}$$

where ρ_{ν} is energy density of one specie of neutrino. Any additional weakly interacting particles moving relativistically such as axions contributes more energy density to the radiation part and this effect can be included inside the definition of N_{eff} as following

$$\begin{aligned} \rho'_{rad} &= \rho_{e^{\pm}} + \rho_{\gamma} + N_{eff}\rho_{\nu} + \rho_{a} \\ &= \rho_{e^{\pm}} + \rho_{\gamma} + N_{eff}\rho_{\nu}\left(1 + \frac{\rho_{a}}{\rho_{3\nu}}\right) \\ \frac{\Delta N_{eff}}{N_{eff}} &= \frac{\rho_{a}}{\rho_{3\nu}} \end{aligned} \tag{A.2}$$

where $\rho_{3\nu}$ is the energy density for 3 species of neutrino. Since both neutrinos and axion are not in thermal equilibrium between the time of neutrino decoupling to the time of BBN (2.5 MeV - 1 MeV), their energy density dilute in exactly the same way. Thus, we have

$$\frac{\rho_a(\text{BBN})}{\rho_{3\nu}(\text{BBN})} = \frac{\rho_a(\nu\text{dec})}{\rho_{3\nu}(\nu\text{dec})} \tag{A.3}$$

At this period, the thermal plasma consists of electrons, positrons, photons and neutrinos with the same temperature. Therefore, one can find the energy density ratio between neutrinos and the standard model radiation from counting the degrees of freedom each components has

$$\begin{aligned} \frac{\rho_{rad}}{\rho_{3\nu}} &= 1 + \frac{\rho_{e^\pm}}{\rho_{3\nu}} + \frac{\rho_\gamma}{\rho_{3\nu}} \\ &= 1 + \frac{2 \times 2 \times 7/8}{3 \times 2 \times 7/8} + \frac{2}{3 \times 2 \times 7/8} \\ &= \frac{43}{21} \end{aligned} \tag{A.4}$$

Putting all relations together, we obtain

$$\begin{aligned} \Delta N_{eff} &= \frac{N_{eff}\rho_a(\text{BBN})}{\rho_{3\nu}(\text{BBN})} \\ &= \frac{3\rho_a(\nu\text{dec})}{\rho_{3\nu}(\nu\text{dec})} \\ &= \frac{43\rho_a(\nu\text{dec})}{7\rho_{rad}(\nu\text{dec})} \end{aligned} \tag{A.5}$$

To make predictions from the moduli branching fractions, we need to relate this quantity to the time of reheating in the moduli decay scenario. Firstly, because of its very weak coupling, axions have never been in thermal equilibrium. As a consequence, its energy density scales as $1/a^4$ where a is the scaling factor. We

can write

$$\frac{\rho_a(\nu\text{dec})}{\rho_a(reheat)} = \frac{a^4(\text{reheat})}{a^4(\nu\text{dec})} \tag{A.6}$$

On the other hand, the standard model radiation part is in the thermal equilibrium from the time of reheating to the time of neutrino decoupling. To find the scaling factor, we use the fact that the comoving entropy is conserved $S \sim a^3 g_\star(T) T^3$. Therefore, we get

$$\begin{aligned} \rho_{rad} &\sim g_\star(T) T^4 \\ &\sim \frac{1}{a^4 g_\star^{1/3}(T)} \\ \frac{\rho_{rad}(\nu\text{dec})}{\rho_{rad}(\text{reheat})} &= \frac{a^4(\text{reheat}) g_\star^{1/3}(\text{reheat})}{a^4(\nu\text{dec}) g_\star^{1/3}(\nu\text{dec})} \end{aligned} \tag{A.7}$$

Substitute (A.6), we obtain

$$\frac{\rho_a(\nu\text{dec})}{\rho_{rad}(\nu\text{dec})} = \frac{\rho_a(\text{reheat})}{\rho_{rad}(\text{reheat})} \frac{g_\star^{1/3}(\nu\text{dec})}{g_\star^{1/3}(\text{reheat})} \tag{A.8}$$

Then, the effective number of neutrinos can be written as

$$\begin{aligned} \Delta N_{eff} &= \frac{43}{7} \frac{\rho_a(\text{reheat})}{\rho_{rad}(\text{reheat})} \frac{g_\star^{1/3}(\nu\text{dec})}{g_\star^{1/3}(\text{reheat})} \\ &= \frac{43}{7} \frac{\text{Br}(X_i \to \text{axions})}{1 - \text{Br}(X_i \to \text{axions})} \frac{g_\star^{1/3}(\nu\text{dec})}{g_\star^{1/3}(\text{reheat})} \end{aligned} \tag{A.9}$$

A.2 The lepton isolation requirement

In hadron colliders, leptons (electrons and muons) may arise from heavy hadron decays. Those "background" leptons are usually found together with other particles around them. The leptons originating from gauge boson decays can therefore

be distinguished from the background leptons by investigating activity around the lepton. For this check, `Delphes 3` uses an isolation variable, I, defined as

$$I(\ell) = \frac{\sum\limits_{i \neq \ell}^{\Delta R < R,\ p_T(i) > p_T^{\min}} p_T(i)}{p_T(\ell)}, \tag{A.10}$$

where the numerator sums the p_T of all particles (except for the lepton itself) with $p_T > p_T^{\min}$ lying within a cone of radius R around the lepton. If $I(\ell)$ is smaller than $I_{\min}$, the lepton is said to be isolated, otherwise it gets rejected as background. The Snowmass samples were generated using `Delphes 3` with the lepton isolation parameters $R = 0.3$, $p_T^{\min} = 0.5$ and $I_{min} = 0.1$.

A 100 TeV collider can explore charginos and neutralinos with their mass scale of a few TeV. If the mass hierarchy between W-ino states and Higgsino states are much higher than the gauge bosons mass scale, the W and Z produced from the W-ino decays will be highly boosted. If such a boosted Z decays into a pair of same-flavour opposite-sign (SFOS) leptons, those two leptons can be highly collimated, and one may be rejected by the isolation criteria defined above.

To see the impact of this effect, we show the $\Delta R_{\rm SFOS}$ (the distance between the SFOS pair[1]) distributions in figure A.1. In figure A.1, the background sample consists of the most relevant processes, WZ and ttZ, which we have generated using `MadGraph 5` and `Phythia 6`.[2] For signal, we examine three benchmark points: $(M_2, \mu)/\text{GeV} =$ (800, 200), (1200, 200) and (1800, 200). The particle level samples are passed to `Delphes 3` with the same detector setup as used in Snowmass but with $R = 0.05$ for the lepton isolation cone radius.

[1] To be explicit, $\Delta R_{\rm SFOS} = \sqrt{(\Delta\phi_{\rm SFOS})^2 + (\Delta\eta_{\rm SFOS})^2}$, where $\Delta\phi_{\rm SFOS}$ and $\Delta\eta_{\rm SFOS}$ are the azimuthal and pseudo-rapidity differences between the SFOS lepton pair.

[2] In the WZ sample, two extra partons are matched with the parton shower radiation with the MLM merging scheme [123].

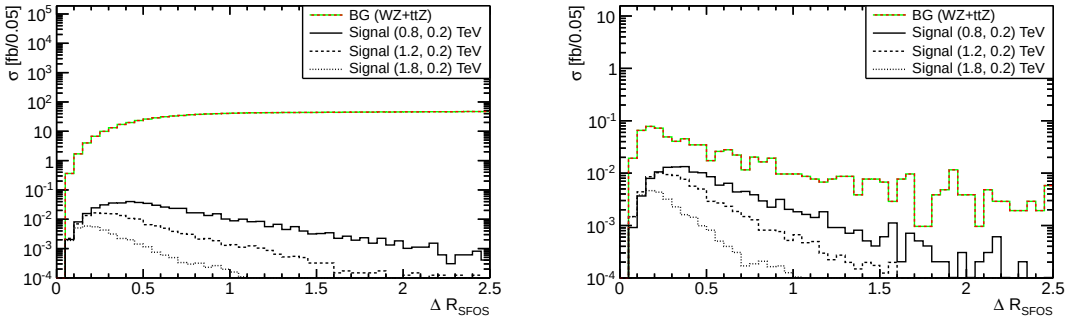

(a) (b)

Figure A.1: The distributions of ΔR_{SFOS}, the distance between the SFOS lepton pair, **(a)** after preselection cuts, **(b)** after additional cuts: $E_T^{\text{miss}} > 500$ GeV and $m_T > 200$ GeV. For both plots, detector simulation has been done by `Delphes 3` using the same detector setup as the one used in Snowmass samples but with $R = 0.05$.

Figure A.1(a) shows the ΔR_{SFOS} distributions after the preselection cuts. As can be seen, signal events are more concentrated around the small ΔR_{SFOS} values, while the background has a rather flat distribution. One can also see that a smaller ΔR_{SFOS} is preferred for model points with larger mass hierarchy.

In Figure A.1(b) we present the same distributions of ΔR_{SFOS} but with the requirement of $E_T^{\text{miss}} > 500$ GeV and $m_T > 200$ GeV on top of the preselection cuts. As can be seen, the distributions are more concentrated for signal and background compared to the distributions with only preselection cuts. This is because the harsh cuts on E_T^{miss} and m_T call for large $\sqrt{\hat{s}}$ for the partonic collision, leading to more boosted Z for both signal and background events. One can see that the significant fraction of events has a SFOS lepton pair lying within $\Delta R_{\text{SFOS}} < 0.3$ of each other, and it is expected that the Snowmass lepton isolation criteria with $R = 0.3$ would reject some fraction of signal and background events. We therefore believe that employing smaller lepton isolation cone radius will improve the

chargino-neutralino mass reach to some extent, although a dedicated study in this direction is beyond the scope of this work.

A.3 The visible cross sections

In this section we report the visible cross sections (the cross section after cuts) for each step of the selection cuts for different processes. Four sets of samples are considered for the SM background, which are defined in table 4.2. We show the results for three benchmark model points for signal: $(M_2, \mu)/\text{GeV} = (800, 200)$, (1200, 200) and (1800, 200). The (visible) cross sections with k-factor = 3 are shown in fb for all tables in this section. Table A.1 shows the (visible) cross sections for the cuts employed in the *preselection* stage. Table A.2, A.3 and A.4 show the visible cross sections for the cuts used in *Loose*, *Medium* and *Tight* signal regions, respectively. The last columns in tables A.2, A.3 and A.4 show $S/\sqrt{B}$ assuming 3000 fb^{-1} of integrated luminosity for the three different benchmark points.

Process	No cut	= 3 lepton	$\lvert m_{\ell\ell}^{\text{SFOS}} - m_Z \rvert < 10$	no-b jet
VV	3025348	2487	2338	2176
ttV	220161	792	552	318
tV	2764638	68.9	6.07	4.12
VVV	36276	76.1	56.2	56.2
BG total	6046422	3424	2952	2554
$(M_2, \mu) = (800, 200)$	1.640	0.588	0.565	0.534
$(M_2, \mu) = (1200, 200)$	0.397	0.124	0.119	0.111
$(M_2, \mu) = (1800, 200)$	0.0863	0.0190	0.0179	0.0170

Table A.1: The (visible) cross sections (in fb) for the cuts employed in the *preselection*. The column marked "No cut" shows the cross sections for the background processes (defined in table 4.2) and the cross section times branching ratio into 3 leptons via WZ for signal benchmark points.

Process	$p_T^\ell > (100, 50, 10)$	$E_T^{\rm miss} > 150$	$m_T > 150$	$S/\sqrt{B}$
VV	647	106	5.1	
ttV	176	41.2	6.6	
tV	0.665	0.391	0.0793	
VVV	23.4	6.0	1.06	
BG total	847	153	12.8	
$(M_2, \mu) = (800, 200)$	0.506	0.465	0.381	5.82
$(M_2, \mu) = (1200, 200)$	0.109	0.103	0.090	1.38
$(M_2, \mu) = (1800, 200)$	0.0168	0.0164	0.0150	0.234

Table A.2: The visible cross sections (in fb) used in the *Loose* signal region. The last column shows $S/\sqrt{B}$ assuming the 3000 fb^{-1} luminosity for different benchmark points.

Process	$p_T^\ell > (250, 150, 50)$	$E_T^{\rm miss} > 350$	$m_T > 300$	$S/\sqrt{B}$
VV	33.8	3.13	0.106	
ttV	9.84	0.780	0.119	
tV	0.037	0.0213	0.00132	
VVV	1.87	0.291	0.0442	
BG total	45.6	4.22	0.271	
$(M_2, \mu) = (800, 200)$	0.170	0.107	0.0845	8.89
$(M_2, \mu) = (1200, 200)$	0.0572	0.0463	0.0408	4.30
$(M_2, \mu) = (1800, 200)$	0.0099	0.0088	0.0081	0.845

Table A.3: The visible cross sections (in fb) used in the *Medium* signal region. The last column shows $S/\sqrt{B}$ assuming the 3000 fb^{-1} luminosity for different benchmark points.

Process	$p_T^\ell > (400, 200, 75)$	$E_T^{\rm miss} > 800$	$m_T > 1100$	$S/\sqrt{B}$
VV	5.65	0.123	0.00166	
ttV	1.03	0.0056	0.00092	
tV	0.015	0.0001	0	
VVV	0.350	0.0109	0.00153	
BG total	7.05	0.140	0.00411	
$(M_2, \mu) = (800, 200)$	0.0460	0.0020	0.0012	1.00
$(M_2, \mu) = (1200, 200)$	0.0238	0.0070	0.0052	4.45
$(M_2, \mu) = (1800, 200)$	0.0053	0.0031	0.0026	2.22

Table A.4: The visible cross sections (in fb) used in the *Tight* signal region. The last column shows $S/\sqrt{B}$ assuming the 3000 fb^{-1} luminosity for different benchmark points.

Bibliography

[1] Gerard Jungman, Marc Kamionkowski, and Kim Griest. Supersymmetric dark matter. Phys. Rept., 267:195–373, 1996.

[2] Keith A. Olive. TASI lectures on dark matter.

[3] Gianfranco Bertone, Dan Hooper, and Joseph Silk. Particle dark matter: Evidence, candidates and constraints. Phys. Rept., 405:279–390, 2005.

[4] Steven Weinberg. The Cosmological Constant Problem. Rev. Mod. Phys., 61:1–23, 1989.

[5] Edward Witten. The Cosmological constant from the viewpoint of string theory.

[6] Sean M. Carroll. The Cosmological constant. Living Rev. Rel., 4:1, 2001.

[7] R. N. Mohapatra et al. Theory of neutrinos: A White paper. Rept. Prog. Phys., 70:1757–1867, 2007.

[8] R. N. Mohapatra and A. Y. Smirnov. Neutrino Mass and New Physics. Ann. Rev. Nucl. Part. Sci., 56:569–628, 2006.

[9] R. D. Peccei. The Strong CP problem and axions. Lect. Notes Phys., 741:3–17, 2008. [,3(2006)].

[10] Jihn E. Kim. A Review on axions and the strong CP problem. AIP Conf. Proc., 1200:83–92, 2010.

[11] Jihn E. Kim and Gianpaolo Carosi. Axions and the Strong CP Problem. Rev. Mod. Phys., 82:557–602, 2010.

[12] Shamit Kachru, Renata Kallosh, Andrei D. Linde, and Sandip P. Trivedi. De Sitter vacua in string theory. Phys. Rev., D68:046005, 2003.

[13] Vijay Balasubramanian, Per Berglund, Joseph P. Conlon, and Fernando Quevedo. Systematics of moduli stabilisation in Calabi-Yau flux compactifications. JHEP, 03:007, 2005.

[14] Frederik Denef, Michael R. Douglas, Bogdan Florea, Antonella Grassi, and Shamit Kachru. Fixing all moduli in a simple f-theory compactification. Adv. Theor. Math. Phys., 9(6):861–929, 2005.

[15] Katrin Becker, Melanie Becker, Cumrun Vafa, and Johannes Walcher. Moduli Stabilization in Non-Geometric Backgrounds. Nucl. Phys., B770:1–46, 2007.

[16] Michael R. Douglas and Shamit Kachru. Flux compactification. Rev. Mod. Phys., 79:733–796, 2007.

[17] Frederik Denef, Michael R. Douglas, and Shamit Kachru. Physics of String Flux Compactifications. Ann. Rev. Nucl. Part. Sci., 57:119–144, 2007.

[18] John Preskill, Mark B. Wise, and Frank Wilczek. Cosmology of the Invisible Axion. Phys. Lett., B120:127–132, 1983.

[19] L. F. Abbott and P. Sikivie. A Cosmological Bound on the Invisible Axion. Phys. Lett., B120:133–136, 1983.

[20] Michael Dine and Willy Fischler. The Not So Harmless Axion. Phys. Lett., B120:137–141, 1983.

[21] Tom Banks, David B. Kaplan, and Ann E. Nelson. Cosmological implications of dynamical supersymmetry breaking. Phys.Rev., D49:779–787, 1994.

[22] B. de Carlos, J.A. Casas, F. Quevedo, and E. Roulet. Model independent properties and cosmological implications of the dilaton and moduli sectors of 4-d strings. Phys.Lett., B318:447–456, 1993.

[23] Bobby Samir Acharya, Piyush Kumar, Konstantin Bobkov, Gordon Kane, Jing Shao, et al. Non-thermal Dark Matter and the Moduli Problem in String Frameworks. JHEP, 0806:064, 2008.

[24] Michael B. Green, J. H. Schwarz, and Edward Witten. Superstring Theory. Vol. 1: Introduction. 1988.

[25] Michael B. Green, J. H. Schwarz, and Edward Witten. Superstring Theory. Vol 2: Loop Amplitudes, Anomalies and phenomenology. 1988.

[26] Maximilian Kreuzer and Harald Skarke. Complete classification of reflexive polyhedra in four-dimensions. Adv. Theor. Math. Phys., 4:1209–1230, 2002.

[27] James Halverson and Washington Taylor. $\mathbb{P}^1$-bundle bases and the prevalence of non-Higgsable structure in 4D F-theory models. JHEP, 09:086, 2015.

[28] Alessio Corti, Mark Haskins, Johannes Nordstrm, and Tommaso Pacini. G_2-manifolds and associative submanifolds via semi-Fano 3-folds. Duke Math. J., 164(10):1971–2092, 2015.

[29] Asimina Arvanitaki, Savas Dimopoulos, Sergei Dubovsky, Nemanja Kaloper, and John March-Russell. String Axiverse. Phys.Rev., D81:123530, 2010.

[30] Bobby Samir Acharya and Konstantin Bobkov. Kahler Independence of the G(2)-MSSM. JHEP, 1009:001, 2010.

[31] Bobby Samir Acharya, Konstantin Bobkov, Gordon L. Kane, Piyush Kumar, and Jing Shao. Explaining the Electroweak Scale and Stabilizing Moduli in M Theory. Phys.Rev., D76:126010, 2007.

[32] Bobby Samir Acharya, Konstantin Bobkov, Gordon L. Kane, Jing Shao, and Piyush Kumar. The G(2)-MSSM: An M Theory motivated model of Particle Physics. Phys.Rev., D78:065038, 2008.

[33] Oskar Klein. Quantum Theory and Five-Dimensional Theory of Relativity. (In German and English). Z. Phys., 37:895–906, 1926. [Surveys High Energ. Phys.5,241(1986)].

[34] Luis E. Ibanez and Angel M. Uranga. String theory and particle physics: An introduction to string phenomenology. Cambridge University Press, 2012.

[35] Theodor Kaluza. On the Problem of Unity in Physics. Sitzungsber. Preuss. Akad. Wiss. Berlin (Math. Phys.), 1921:966–972, 1921.

[36] P. Candelas, Gary T. Horowitz, Andrew Strominger, and Edward Witten. Vacuum Configurations for Superstrings. Nucl. Phys., B258:46–74, 1985.

[37] G. Papadopoulos and P. K. Townsend. Compactification of D = 11 supergravity on spaces of exceptional holonomy. Phys. Lett., B357:300–306, 1995.

[38] Bobby Samir Acharya and Sergei Gukov. M theory and singularities of exceptional holonomy manifolds. Phys.Rept., 392:121–189, 2004.

[39] Philip Candelas and Xenia de la Ossa. Moduli Space of Calabi-Yau Manifolds. Nucl. Phys., B355:455–481, 1991.

[40] Savas Dimopoulos and Howard Georgi. Softly Broken Supersymmetry and SU(5). Nucl. Phys., B193:150–162, 1981.

[41] Savas Dimopoulos. Soft supersymmetry breaking and the supersymmetric standard model. Nucl. Phys. Proc. Suppl., 101:183–194, 2001. [,183(2001)].

[42] D. J. H. Chung, L. L. Everett, G. L. Kane, S. F. King, Joseph D. Lykken, and Lian-Tao Wang. The Soft supersymmetry breaking Lagrangian: Theory and applications. Phys. Rept., 407:1–203, 2005.

[43] Jihn E. Kim and Hans Peter Nilles. The mu Problem and the Strong CP Problem. Phys. Lett., B138:150–154, 1984.

[44] G.F. Giudice and A. Masiero. A Natural Solution to the mu Problem in Supergravity Theories. Phys.Lett., B206:480–484, 1988.

[45] Bobby Samir Acharya, Gordon Kane, Eric Kuflik, and Ran Lu. Theory and Phenomenology of μ in M theory. JHEP, 1105:033, 2011.

[46] Bobby Samir Acharya and Chakrit Pongkitivanichkul. The Axiverse induced Dark Radiation Problem. JHEP, 04:009, 2016.

[47] Bobby S. Acharya, Krzysztof Bo?ek, Miguel Crispim Romo, Stephen F. King, and Chakrit Pongkitivanichkul. SO(10) Grand Unification in M theory on a G2 manifold. Phys. Rev., D92(5):055011, 2015.

[48] Bobby S. Acharya, Krzysztof Bo?ek, Chakrit Pongkitivanichkul, and Kazuki Sakurai. Prospects for observing charginos and neutralinos at a 100 TeV proton-proton collider. JHEP, 02:181, 2015.

[49] Peter Svrcek and Edward Witten. Axions In String Theory. JHEP, 0606:051, 2006.

[50] Bobby Samir Acharya, Konstantin Bobkov, and Piyush Kumar. An M Theory Solution to the Strong CP Problem and Constraints on the Axiverse. JHEP, 1011:105, 2010.

[51] George Lazarides, Robert K. Schaefer, D. Seckel, and Q. Shafi. Dilution of Cosmological Axions by Entropy Production. Nucl. Phys., B346:193–212, 1990.

[52] Patrick Fox, Aaron Pierce, and Scott D. Thomas. Probing a QCD string axion with precision cosmological measurements. 2004.

[53] Jared Kaplan. Dark matter generation and split supersymmetry. JHEP, 10:065, 2006.

[54] G. Hinshaw et al. Nine-Year Wilkinson Microwave Anisotropy Probe (WMAP) Observations: Cosmological Parameter Results. 2012.

[55] Z. Hou, C.L. Reichardt, K.T. Story, B. Follin, R. Keisler, et al. Constraints on Cosmology from the Cosmic Microwave Background Power Spectrum of the 2500-square degree SPT-SZ Survey. 2012.

[56] Jonathan L. Sievers, Renee A. Hlozek, Michael R. Nolta, Viviana Acquaviva, Graeme E. Addison, et al. The Atacama Cosmology Telescope: Cosmological parameters from three seasons of data. 2013.

[57] P. A. R. Ade et al. Planck 2015 results. XIII. Cosmological parameters. 2015.

[58] Michele Cicoli, Joseph P. Conlon, and Fernando Quevedo. Dark Radiation in LARGE Volume Models. Phys.Rev., D87:043520, 2013.

[59] Tetsutaro Higaki and Fuminobu Takahashi. Dark Radiation and Dark Matter in Large Volume Compactifications. JHEP, 1211:125, 2012.

[60] Tetsutaro Higaki, Kazunori Nakayama, and Fuminobu Takahashi. Moduli-Induced Axion Problem. JHEP, 1307:005, 2013.

[61] Joseph P. Conlon and M. C. David Marsh. The Cosmophenomenology of Axionic Dark Radiation. JHEP, 1310:214, 2013.

[62] Stephen Angus, Joseph P. Conlon, Ulrich Haisch, and Andrew J. Powell. Loop corrections to ΔN_{eff} in large volume models. JHEP, 12:061, 2013.

[63] Michele Cicoli. Axion-like Particles from String Compactifications. 2013.

[64] Michele Cicoli, Joseph P. Conlon, M. C. David Marsh, and Markus Rummel. 3.55 keV photon line and its morphology from a 3.55 keV axionlike particle line. Phys. Rev., D90:023540, 2014.

[65] Stephen Angus. Dark Radiation in Anisotropic LARGE Volume Compactifications. JHEP, 1410:184, 2014.

[66] Arthur Hebecker, Patrick Mangat, Fabrizio Rompineve, and Lukas T. Witkowski. Dark Radiation predictions from general Large Volume Scenarios. JHEP, 1409:140, 2014.

[67] Michele Cicoli and Francesco Muia. General Analysis of Dark Radiation in Sequestered String Models. 2015.

[68] David J. E. Marsh. Axion Cosmology. 2015.

[69] Joseph P. Conlon, Fernando Quevedo, and Kerim Suruliz. Large-volume flux compactifications: Moduli spectrum and D3/D7 soft supersymmetry breaking. JHEP, 08:007, 2005.

[70] Bobby Samir Acharya, Gordon Kane, and Piyush Kumar. Compactified String Theories – Generic Predictions for Particle Physics. Int.J.Mod.Phys., A27:1230012, 2012.

[71] Edward Witten. Symmetry Breaking Patterns in Superstring Models. Nucl.Phys., B258:75, 1985.

[72] Rabindra N. Mohapatra and Michael Ratz. Gauged Discrete Symmetries and Proton Stability. Phys.Rev., D76:095003, 2007.

[73] Hyun Min Lee, Stuart Raby, Michael Ratz, Graham G. Ross, Roland Schieren, et al. A unique Z_4^R symmetry for the MSSM. Phys.Lett., B694:491–495, 2011.

[74] Edward Witten. Deconstruction, G(2) holonomy, and doublet triplet splitting.

[75] A. Brignole, Luis E. Ibanez, and C. Munoz. Soft supersymmetry breaking terms from supergravity and superstring models. Adv. Ser. Direct. High Energy Phys., 21:244–268, 2010.

[76] J. Wess and J. Bagger. Supersymmetry and supergravity. 1992.

[77] G.R. Dvali. Light color triplet Higgs is compatible with proton stability: An Alternative approach to the doublet - triplet splitting problem. Phys.Lett., B372:113–120, 1996.

[78] Wolfgang Kilian and Jurgen Reuter. Unification without doublet-triplet splitting. Phys.Lett., B642:81–84, 2006.

[79] Juergen Reuter. SUSY multi-step unification without doublet-triplet splitting. 2007.

[80] R. Howl and S.F. King. Minimal E(6) Supersymmetric Standard Model. JHEP, 0801:030, 2008.

[81] Christopher F. Kolda and Stephen P. Martin. Low-energy supersymmetry with D term contributions to scalar masses. Phys. Rev., D53:3871–3883, 1996.

[82] Bobby Samir Acharya and Edward Witten. Chiral fermions from manifolds of G(2) holonomy. 2001.

[83] Takeshi Araki, Tatsuo Kobayashi, Jisuke Kubo, Saul Ramos-Sanchez, Michael Ratz, et al. (Non-)Abelian discrete anomalies. Nucl.Phys., B805:124–147, 2008.

[84] Bobby S. Acharya, Gordon L. Kane, Piyush Kumar, Ran Lu, and Bob Zheng. R-Parity Conservation from a Top Down Perspective. JHEP, 1410:1, 2014.

[85] Tom Banks, Yuval Grossman, Enrico Nardi, and Yosef Nir. Supersymmetry without R-parity and without lepton number. Phys.Rev., D52:5319–5325, 1995.

[86] Herbert K. Dreiner. An Introduction to explicit R-parity violation. Adv.Ser.Direct.High Energy Phys., 21:565–583, 2010.

[87] Bobby S. Acharya, Sebastian A. R. Ellis, Gordon L. Kane, Brent D. Nelson, and Malcolm J. Perry. The lightest visible-sector supersymmetric particle is likely to be unstable. 2016.

[88] Georges Aad et al. Search for direct production of charginos, neutralinos and sleptons in final states with two leptons and missing transverse momentum in pp collisions at $\sqrt{s} = 8$ TeV with the ATLAS detector. JHEP, 1405:071, 2014.

[89] Vardan Khachatryan et al. Searches for electroweak production of charginos, neutralinos, and sleptons decaying to leptons and W, Z, and Higgs bosons in pp collisions at 8 TeV. 2014.

[90] Search for Supersymmetry at the high luminosity LHC with the ATLAS experiment. Technical Report ATL-PHYS-PUB-2014-010, CERN, Geneva, 2014.

[91] Timothy Cohen, Tobias Golling, Mike Hance, Anna Henrichs, Kiel Howe, et al. SUSY Simplified Models at 14, 33, and 100 TeV Proton Colliders. JHEP, 1404:117, 2014.

[92] Tim Andeen, Clare Bernard, Kevin Black, Taylor Childres, Lidia Dell'Asta, et al. Sensitivity to the Single Production of Vector-Like Quarks at an Upgraded Large Hadron Collider. 2013.

[93] Leonard Apanasevich, Suneet Upadhyay, Nikos Varelas, Daniel Whiteson, and Felix Yu. Sensitivity of potential future *pp* colliders to quark compositeness. 2013.

[94] Daniel Stolarski. Reach in All Hadronic Stop Decays: A Snowmass White Paper. 2013.

[95] Felix Yu. Di-jet resonances at future hadron colliders: A Snowmass whitepaper. 2013.

[96] Ning Zhou, David Berge, LianTao Wang, Daniel Whiteson, and Tim Tait. Sensitivity of future collider facilities to WIMP pair production via effective operators and light mediators. 2013.

[97] Sunghoon Jung and James D. Wells. Gaugino physics of split supersymmetry spectrum at the LHC and future proton colliders. Phys.Rev., D89:075004, 2014.

[98] Andrew Fowlie and Martti Raidal. Prospects for constrained supersymmetry at $\sqrt{s} = 33\,\mathrm{TeV}$ and $\sqrt{s} = 100\,\mathrm{TeV}$ proton-proton super-colliders. Eur.Phys.J., C74:2948, 2014.

[99] Sebastian A. R. Ellis, Gordon L. Kane, and Bob Zheng. Superpartners at LHC and Future Colliders: Predictions from Constrained Compactified M-Theory. 2014.

[100] Matthew Low and Lian-Tao Wang. Neutralino Dark Matter at 100 TeV. 2014.

[101] Marco Cirelli, Filippo Sala, and Marco Taoso. Wino-like Minimal Dark Matter and future colliders. 2014.

[102] David Curtin, Patrick Meade, and Chiu-Tien Yu. Testing Electroweak Baryogenesis with Future Colliders. JHEP, 1411:127, 2014.

[103] Lisa Randall and Raman Sundrum. Out of this world supersymmetry breaking. Nucl.Phys., B557:79–118, 1999.

[104] Gian F. Giudice, Markus A. Luty, Hitoshi Murayama, and Riccardo Rattazzi. Gaugino mass without singlets. JHEP, 9812:027, 1998.

[105] Takeo Moroi and Lisa Randall. Wino cold dark matter from anomaly mediated SUSY breaking. Nucl.Phys., B570:455–472, 2000.

[106] Nima Arkani-Hamed and Savas Dimopoulos. Supersymmetric unification without low energy supersymmetry and signatures for fine-tuning at the LHC. JHEP, 0506:073, 2005.

[107] G.F. Giudice and A. Romanino. Split supersymmetry. Nucl.Phys., B699:65–89, 2004.

[108] N. Arkani-Hamed, S. Dimopoulos, G.F. Giudice, and A. Romanino. Aspects of split supersymmetry. Nucl.Phys., B709:3–46, 2005.

[109] Michele Cicoli, Joseph P. Conlon, and Fernando Quevedo. General Analysis of LARGE Volume Scenarios with String Loop Moduli Stabilisation. JHEP, 10:105, 2008.

[110] J. Alwall, R. Frederix, S. Frixione, V. Hirschi, F. Maltoni, et al. The automated computation of tree-level and next-to-leading order differential cross sections, and their matching to parton shower simulations. JHEP, 1407:079, 2014.

[111] Sunghoon Jung. Resolving the existence of Higgsinos in the LHC inverse problem. JHEP, 1406:111, 2014.

[112] A. Djouadi, M.M. Muhlleitner, and M. Spira. Decays of supersymmetric particles: The Program SUSY-HIT (SUspect-SdecaY-Hdecay-InTerface). Acta Phys.Polon., B38:635–644, 2007.

[113] Howard Baer, Vernon Barger, Andre Lessa, Warintorn Sreethawong, and Xerxes Tata. Wh plus missing-E_T signature from gaugino pair production at the LHC. Phys.Rev., D85:055022, 2012.

[114] T. Han, S. Padhi, and S. Su. Electroweakinos in the Light of the Higgs Boson. Phys.Rev., D88:115010, 2013.

[115] Diptimoy Ghosh, Monoranjan Guchait, and Dipan Sengupta. Higgs Signal in Chargino-Neutralino Production at the LHC. Eur.Phys.J., C72:2141, 2012.

[116] Pritibhajan Byakti and Diptimoy Ghosh. Magic Messengers in Gauge Mediation and signal for 125 GeV boosted Higgs boson. Phys.Rev., D86:095027, 2012.

[117] Andreas Papaefstathiou, Kazuki Sakurai, and Michihisa Takeuchi. Higgs boson to di-tau channel in Chargino-Neutralino searches at the LHC. 2014.

[118] Jacob Anderson, Aram Avetisyan, Raymond Brock, Sergei Chekanov, Timothy Cohen, et al. Snowmass Energy Frontier Simulations. 2013.

[119] Patrick Meade and Matthew Reece. BRIDGE: Branching ratio inquiry / decay generated events. 2007.

[120] Torbjorn Sjostrand, Stephen Mrenna, and Peter Z. Skands. PYTHIA 6.4 Physics and Manual. JHEP, 0605:026, 2006.

[121] J. de Favereau et al. DELPHES 3, A modular framework for fast simulation of a generic collider experiment. JHEP, 1402:057, 2014.

[122] Stefania Gori, Sunghoon Jung, Lian-Tao Wang, and James D. Wells. Prospects for Electroweakino Discovery at a 100 TeV Hadron Collider. 2014.

[123] Michelangelo L. Mangano, Mauro Moretti, Fulvio Piccinini, and Michele Treccani. Matching matrix elements and shower evolution for top-quark production in hadronic collisions. JHEP, 0701:013, 2007.